



HAL
open science

Synthesis, Fluorescence, and Two-Photon Absorption of a Series of Elongated Rodlike and Banana-Shaped Quadrupolar Fluorophores: A Comprehensive Study of Structure–Property Relationships

Olivier Mongin, Laurent Porrès, Marina Charlot, Claudine Katan, Mireille Blanchard-Desce

► To cite this version:

Olivier Mongin, Laurent Porrès, Marina Charlot, Claudine Katan, Mireille Blanchard-Desce. Synthesis, Fluorescence, and Two-Photon Absorption of a Series of Elongated Rodlike and Banana-Shaped Quadrupolar Fluorophores: A Comprehensive Study of Structure–Property Relationships. *Chemistry - A European Journal*, 2007, 13 (5), pp.1481-1498. 10.1002/chem.200600689 . hal-00516962v2

HAL Id: hal-00516962

<https://hal.science/hal-00516962v2>

Submitted on 15 Dec 2016

HAL is a multi-disciplinary open access archive for the deposit and dissemination of scientific research documents, whether they are published or not. The documents may come from teaching and research institutions in France or abroad, or from public or private research centers.

L'archive ouverte pluridisciplinaire **HAL**, est destinée au dépôt et à la diffusion de documents scientifiques de niveau recherche, publiés ou non, émanant des établissements d'enseignement et de recherche français ou étrangers, des laboratoires publics ou privés.

Synthesis, Fluorescence and Two-Photon Absorption of a Series of Elongated Rod-like and Banana-shaped Quadrupolar Fluorophores: a Comprehensive Study of Structure-Property Relationships

Olivier Mongin,* Laurent Porrès, Marina Charlot, Claudine Katan, Mireille Blanchard-Desce*^[a]

Abstract: An extensive series of push-push and pull-pull derivatives was prepared from the symmetrical functionalization of an ambivalent core with conjugated rods made from arylene-vinylene or arylene-ethynylene building blocks, bearing different acceptor or donor end-groups. Their absorption and photoluminescence as well as their two-photon absorption (TPA) properties in the near infrared (NIR) region have been systematically investigated in order to derive structure-property relationships and lay the guidelines for both spectral tuning and amplification of molecular TPA in the target region. Whatever the nature of the core or of the connectors, push-push systems were found to be more efficient than pull-pull systems and planarization of the core (fluorene vs biphenyl) always leads to an increase of the TPA cross-sections. At contrary, increasing the conjugation length as well as replacement of a phenylene moiety by a thienylene moiety in the conjugated rods *did not* necessarily lead to increased TPA responses. The present study also demonstrated that the topology of the conjugated rods can dramatically influence the TPA properties. This is of particular interest in terms of molecular engineering for specific applications since both TPA properties and photoluminescence characteristics can be considerably affected. It thus becomes possible to optimize the transparency/TPA and fluorescence/TPA efficiency trade-offs, for optical limiting in the red-NIR region (700-900 nm) and TPEF microscopy applications, respectively.

Keywords: chromophores · fluorescence · two-photon absorption · nonlinear optics

^[a] Dr. O. Mongin, Dr. L. Porrès, Dr. M. Charlot, Dr. C. Katan, Dr. M. Blanchard-Desce
Synthèse et ElectroSynthèse Organiques (CNRS, UMR 6510), Institut de Chimie
Université de Rennes 1, Campus Scientifique de Beaulieu, Bât 10A
F-35042 Rennes Cedex (France)
E-mail: mireille.blanchard-desce@univ-rennes1.fr; olivier.mongin@univ-rennes1.fr

Introduction

Molecular two-photon absorption (TPA) has been attracting growing interest over recent years owing to its applications in various fields including spectroscopy,^[1, 2] three-dimensional optical data storage,^[3-7] microfabrication,^[8-11] laser up-conversion,^[12, 13] high-resolution 3-dimensional imaging of biological systems,^[14-17] and photodynamic therapy.^[18] Among these, two-photon-excited fluorescence (TPEF) has gained widespread popularity in the biology community and given rise to the technique of two-photon laser scanning fluorescence microscopy,^[14-16] allowing for instance *in vivo* imaging of calcium dynamics^[17, 19-21] or intracellular zinc.^[22, 23] Using a two-photon excitation process (i.e. a nonlinear process involving the *simultaneous* absorption of two photons) instead of a conventional one-photon excitation actually offers a number of advantages. These include the ability for a highly confined excitation and intrinsic three-dimensional resolution in microscopic imaging. Moreover, by replacing one-photon excitation in the UV-visible blue region by two-photon-excitation in the visible red-near IR region (typically 700-1200 nm), TPEF offers the advantage of imaging at an increased penetration depth in tissues (owing in particular to a reduction of scattering losses) with reduced photodamage as well as improved signal to noise ratio (owing to reduced background fluorescence). The fast development of TPEF microscopy has triggered the search for novel fluorophores specifically engineered for TPEF. Fluorophores having TPA cross-sections many orders of magnitude larger than endogenous fluorophores (such as fluorescent amino-acids, flavins, etc...)^[24-26] are attractive for reducing background fluorescence by *selective* two-photon excitation of TPEF probes. In addition TPEF fluorophores with both broad and intense TPA bands are also of interest because of the versatility they offer in terms of excitation sources (insofar as costly tunable short-pulses laser can be replaced by less expensive non tunable laser sources).

Multiphoton absorption has also attracted considerable attention for optical limiting^[27-39] mainly focusing on optical limiting in the visible region aiming at eye-protection.^[37-39] Whereas a number of multiphoton chromophores have been designed and studied in that context, only scarce effort has been dedicated to the protection of NIR detectors typically working in the 700-900 nm region. Chromophores combining full transparency and strong multiphoton absorptivities (such as overlapping of strong two-photon and excited-state absorptions) in that spectral range are thus required.

Within this context, we have implemented a molecular engineering approach towards elongated rod-like or banana-shaped fluorophores with enhanced TPA cross sections (σ_2) in the target spectral window (i.e. 700-1000 nm).^[40] A high fluorescence quantum yield (Φ) is required for TPEF applications whereas a full linear transparency is required for optical limiting applications. In the present paper, we describe and discuss their molecular design, synthesis, photophysical and TPA properties. A wide scope of molecules has been prepared and investigated in order to derive structure-property relationships and lay the guidelines for both spectral tuning of both absorption and fluorescence and amplification of molecular TPA.

Following the route for molecular TPA optimization opened by Marder and collaborators,^[41, 42] we focused on the optimization of quasi one-dimensional quadrupolar systems, i.e. symmetrical conjugated molecules bearing two electron-releasing (D) or electron-withdrawing (A) end-groups.^[40, 43-45] Indeed quadrupolar systems^[27, 30, 35, 39-79] have been found to be more efficient than push-pull systems^[13, 28, 46, 47, 56, 64, 68, 80-88] in terms of TPA in particular for multiphoton-based optical limiting applications.^[27, 30, 39] Such derivatives can display very high TPA cross sections in connection with a quadrupolar intramolecular charge transfer taking place between the ends and the center of the molecules.^[42] Very large σ_2 values have been obtained with DAAD, ADDA, DADAD, DDADD... systems having strong D and A moieties but often at the cost of reduced fluorescence quantum yield and/or pronounced red-shift of the one-photon absorption band.^[41, 77] In this context, our purpose has been the design of optimized systems displaying enhanced σ_2 values in the red-NIR region (700-1000 nm), while maintaining high fluorescence quantum yields. Our strategy, founded on a three-VB state model,^[89-91] was based on the push-push or pull-pull functionalization of a semi-rigid conjugated system.^[40, 43-45]

Figure 1

The structure was built from the symmetrical grafting, onto a conjugated core, of two elongated conjugated rods bearing either a D or A end-group (Figure 1). The central building blocks were selected as more or less rigid units that may assist quadrupolar intramolecular charge transfer by acting either as a (weak) donor or acceptor core. We selected biphenyl (BP) or fluorene (Fl) central units, which allow the tuning of the electronic delocalization along the conjugated backbone in the ground state by modulation of the twist angle between the two half of the molecules.^[40] It should be noted that the fluorene building block has been

successfully used in the design of both dipolar^[46, 83] or quadrupolar systems with large multiphoton absorption,^[40, 59, 69] owing to the planarity it provides. Conjugated rods built from arylene-ethynylene and/or arylene-vinylene oligomers were investigated in order to maintain fluorescence and modulate the electronic communication between the end-groups and the core of the molecules. The aim of these systematic structural variations was both to derive comprehensive structure-TPA relationships and to ascertain the appropriate combination of core, linker (double versus triple bond) and connector (phenylene P, thienylene T, furylene F, fluorenylene Fl) moieties for optimized TPA/luminescence and/or TPA/transparency properties. Long alkyl chains were grafted on the peripheral groups and/or on the core in order to obtain highly soluble derivatives, which are required for optical limiting application. Moreover, the central nonyl chains on the fluorenyl core were meant to hinder π -stacking and aggregation processes that are detrimental to TPA^[79] and photoluminescence properties.

Results and discussion

Synthesis

The assembly of cores, linkers and end-groups was performed by means of Sonogashira or Heck couplings and Wittig or Horner-Wadsworth-Emmons condensations. Amino (**1a**) and dialkylamino (**1b**)^[92] moieties bearing an iodo group were used as electron-releasing building blocks, and **1b** was also converted to the extended rigid moieties **2a** and **2b** in three-step sequences: (i) palladium(II)-catalyzed reaction with 2-methyl-3-butyn-2-ol, (ii) base-promoted deprotection, and (iii) cross-coupling with 1,4-diiodobenzene and 4-bromobenzaldehyde, respectively (Scheme 1). Other electron-donating dialkylamino building blocks were prepared, bearing either a formyl (**1e**)^[93] or a phosphonium (**3a-c**)^[94] group. Phosphonium salts **3b** and **3c** were also converted to the semi-rigid stilbene rods **4b** and **4a**, respectively, through their Wittig condensation with terephthalaldehyde mono-(diethylacetal) and 4-iodobenzaldehyde, respectively. The furylenevinylene- and thienylenevinylene-containing building blocks **6a-c** were obtained by reaction of 2,5-furanedicarboxaldehyde monoacetal (**5a**)^[95] or 2,5-thiophenedicarboxaldehyde monoacetal (**5b**)^[96] with phosphonium salts **3b** or **3c**, followed by acidic hydrolysis of the intermediate acetals (Scheme 1). The electron-withdrawing alkylsulfone **8a** was prepared by oxidation of thioether **7a**,^[97] while the trifluoromethylsulfone **8d** was obtained from **7b** in a three-step sequence, involving

oxidation, palladium(II)-catalyzed reaction with ethynyltrimethylsilane and cleavage of the trimethylsilyl group. Phosphonates **9a**^[98] and **9b**, as well as phenylenevinylene-extended phosphonate **11**,^[99] were also used as electron-withdrawing moieties. The halogen-bearing sulfone **10** was obtained from a Horner-Wadsworth-Emmons condensation between **9b** and 4-iodobenzaldehyde (Scheme 2).

The synthesis of the biphenyl-cored fluorophores **13a**, **13b** and **14** was achieved by means of a double Sonogashira coupling of **12**^[100] with **1b**, **2a** and **4a**, respectively (Scheme 3). Bisphosphonate **15b** (prepared by Michaelis-Arbusov reaction of 4,4'-bis(bromomethyl)-1,1'-biphenyl (**15a**)^[101] with triethylphosphite) was used to prepare the other biphenyl-cored fluorophores **16a**, **16b**, **17a** and **17b**, by condensation with aldehydes **1e**, **2b**, **6a** and **6c**, respectively (Scheme 3).

The fluorene core **18d** was obtained from 9,9-dinonylfluorene (**18a**) in a three-step sequence: (i) diiodination, (ii) cross-coupling with 2-methyl-3-butyn-2-ol, and (iii) base-promoted deprotection (Scheme 4). Double Sonogashira coupling of **18d** with **1b**, **2a**, and **4a** afforded push-push molecules **19a**, **19b** and **20**, respectively, whereas reaction with **8a** and **10** gave pull-pull molecules **21a** and **21c**, respectively. The bis-trifluoromethylsulfone **21b** was obtained by reacting the diiodo fluorene core **18b** and the alkyne **8d** (Scheme 4).

From 9,9-dinonylfluorene (**18a**) was also obtained the bisaldehyde core **22b**, by successive dibromination, double bromine-lithium exchange and formylation reactions (Scheme 5). Wittig condensation of bisaldehyde **22b** with two equivalents of 4-(methoxybenzyl)triphenylphosphonium bromide gave (after isomerization with a catalytic amount of iodine under illumination) fluorophore **23**, whereas the same reaction with one single equivalent of phosphonium salt **3a** led to the formation of fluorophore **24** together with the new extended building block **25**. Vinylic bis-sulfones **26a** and **26b** were synthesized by a double Horner-Wadsworth-Emmons condensation of the same bisaldehyde **22b** with phosphonates **9a** and **11**, respectively (Scheme 5).

The bisvinyl fluorene core **27**, obtained by condensation of **22b** with methyltriphenylphosphonium iodide, was reacted with 4-iodoaniline **1a** to afford fluorophore **28**, by means of a double Heck-type coupling under Jeffery's^[102] conditions (Scheme 6).

Conversion of **22b** to the fluorenebisphosphonate **29c** was achieved in a three-step sequence (reduction, bromination and Michaelis-Arbusov reaction). At last, this new fluorene core was reacted with aldehydes **4b**, **6b** and **25** in the presence of sodium hydride to give

phenylenevinylene-linked fluorophore **30**, its thienylenevinylene analogue **31** and the trimeric fluorenylene-vinylene **32**, respectively (Scheme 7).

Finally, the bisaldehyde core **22b** and its thienylenevinylene-extended analogue **33**, obtained by reaction of bisphosphonate **29c** with **5b**, afforded fluorophores **34a** and **34b**, respectively, from double Wittig condensations with [[5-(1-piperidinyl)-2-thienyl]methyl]triphenylphosphonium iodide (Scheme 8).

All new fluorophores have been fully characterized by NMR, HRMS and/or elemental analysis. The ^1H and ^{13}C NMR spectra confirm their high symmetry. In addition, their *all-E* stereochemistry was derived from the values of the 3J coupling constants between vinylic protons ($J \sim 16$ Hz). All the dinonylfluorene derivatives are extremely soluble in chlorinated solvents (typically higher than 500 g.L^{-1}) as well as in THF and toluene, whereas the extended biphenyl fluorophores (**13b**, **14**, **16b**) exhibit much lower solubilities ($1\text{--}5 \text{ g.L}^{-1}$). Long alkyl chains located on the central cores are more efficient in increasing the solubility than those located on the peripheral groups. Moreover, the latter are unnecessary when nonyl chains are present on the core, as exemplified with methylsulfonyl derivatives **26a,b**, the solubility of which is quite similar to that of the other dinonylfluorene derivatives.

Absorption and photoluminescence properties

The photophysical properties (absorption and fluorescence) of the new series of fluorophores are collected in Table 1, including fluorescence quantum yields and lifetimes. We observe that all fluorophores display an intense absorption in the near UV-visible blue region with typical molar extinction coefficients ranging from 60,000 to 180,000 $\text{mol}^{-1}\text{.L.cm}^{-1}$. Their absorption and emission range can be tuned by playing on the nature of the end-groups, of the core moiety and on the nature and length of the conjugated rods. In addition, all molecules exhibit good fluorescence quantum yields, ranging between 0.45 and 0.98 (Table 1).

Core effect

Substitution of the biphenyl core by a fluorene core produces a systematic red shift of the absorption band while maintaining quasi identical fluorescence properties (Table 1, Figure 2). Thus, the resulting Stokes shift is consistently reduced. Moreover, except for compounds **14** and **20**, the halfbandwidth of fluorenyl derivatives is systematically smaller than the one of its

biphenyl analogue. In fact, these distinctive features are directly related to geometrical properties: while the fluorene core is already planar in the ground state, the biphenyl unit has some torsional flexibility, the lowest energy conformation corresponding to a twist angle of about 35°. [73] This leads to both blue shift and broadening of the absorption band of biphenyl derivatives when compared to fluorene analogues. The similarities of the emission properties clearly demonstrate that the biphenyl core becomes planar in the relaxed emitting excited state.

Figure 2

Connector effect: phenylene-vinylene versus phenylene-ethynylene

Changing the nature of the conjugated linker allows spectral tuning of both the absorption and emission characteristics (Table 1). Replacing a triple bond by a double bond induces a bathochromic shift and hyperchromic effect of both the absorption and emission bands, in agreement with an extended electronic conjugation in the ground and excited-states (Figure 3). Interestingly, the fluorescence lifetime always increases, most likely in relation with the higher stretching frequency of a C≡C bond with respect to that of a C=C bond, that is responsible for more efficient non-radiative decay.

On the other hand, replacement of a triple bond by a double bond in elongated derivatives (PE₂) produces very different effects on the fluorescence quantum yield depending on its location in the conjugated rods (Table 1). For instance the shorter derivatives (i.e. connectors = PE and PV) show similar fluorescence quantum yields. For the longer derivatives, the replacement of a triple bond by a double bond does not significantly affect the fluorescence quantum yield when the substituted triple bond is positioned next to the central block (i.e. connector = PE-PV instead of PE₂) but a decrease of 25-40% in the fluorescence quantum yield is obtained when the double bond is located close to the end-groups (i.e. linker PV-PE instead of PE₂). [103] This demonstrates that subtle change in the topology of the conjugated rods may strongly influence the photoluminescence efficiency of the series of quadrupolar fluorophores investigated in the present work. Interestingly, further replacement of a triple bond by a double bond (i.e. connector = PV₂) restores high fluorescence quantum yields.

Figure 3

Connector effect: influence of arylene moieties

Replacing a phenyl unit by a thienyl unit in the conjugated connectors always induces a significant bathochromic shift of the emission band but leads either to a blue shift (PV versus TV and PV-TV versus TV2) or a red shift (PV2 versus PV-TV or TV2) of the absorption band (Figure 4), indicating that the reduction of the aromaticity in the connectors does not necessarily lead to a reduction of the electronic gap between the ground and excited-states. On the other hand, the introduction of the low-aromaticity thiophene heterocycle in the conjugated systems always results in lower fluorescence quantum yields. In most cases, larger Stokes shifts are observed but no major nor regular effects are visible on the fluorescence lifetime. This can be related to the combination of slower radiative decays, related to the red-shifted emission, and greater non-radiative decay due to enlarged intersystem crossing.^[104]

Figure 4

Length effect

Increasing the connector length induces a systematic but more or less pronounced red shift and hyperchromic effect of the absorption bands (Table 1). On the other hand, other photoluminescence characteristics are differently affected depending on the nature of the connector. When increasing the length by doubling the same connector (Figure 5, Table 1), absorption bands undergo a broadening and emission bands are red shifted. Since the hyperchromic effect tends to increase the radiative decay whereas the emission red-shift has an opposite effect, the fluorescence quantum yields increase (compound **30** versus **24**) when the former effect dominates whereas the opposite is observed when the latter dominates (compound **26b** versus **26a**). In the case of thienylene-vinylene oligomers, increasing the number of thienylene-vinylene units results in the largest red-shifts of both the absorption and emission bands, as well as to a hyperchromic effect of the absorption band (Figure 5b). The fluorescence quantum yield is maintained but its lifetime decreases by about 30%, in relation with the combination of faster radiative (in relation with the hyperchromic effect) and non-radiative constants (Table 1). In comparison, the lengthening of the conjugated rods based on phenylene-ethynylene oligomers leads to a definite hyperchromic effect but only slight bathochromic shift of the absorption bands (Figure 5c). Similarly to phenylene-vinylene oligomers a red shift of the emission bands is observed whereas the fluorescence quantum yields are maintained or decrease only slightly.

Figure 5

Insertion of thienylene-vinylene, furylene-vinylene or fluorene-vinylene leads to bathochromic shift of both the absorption and emission bands (Figure 6). We note that the fluorene-vinylene leads to the smallest red-shift and highest fluorescence quantum yield whereas the thienylene-vinylene unit leads to the largest red-shift and lowest quantum yield, most probably in relation with increased non-radiative decay due to enlarged intersystem crossing. Interestingly, the furylene-vinylene unit leads to a significantly longer fluorescence lifetime, most probably in relation with a reduction of the radiative decay due to the marked red-shift of the absorption band which is not compensated by hyperchromic effect of the absorption band, as well as to higher Stokes shifts as compared to other conjugating units (Table 1).

Figure 6

End-groups' effect

Finally, we note that increasing either the electron-withdrawing (Figure 7a) or electron-releasing (Figure 7b) character of the peripheral groups leads to a bathochromic shift of both the absorption and emission bands indicative of a more pronounced either core-to-periphery or periphery-to-core intramolecular charge transfer. This indicates that the core can act as either an acceptor^[105] or a donor moiety^[106] depending on the peripheral counterparts. This has been confirmed by molecular orbital calculations.

We observe that pull-pull compounds appear blue-shifted as compared to push-push derivatives (Table 1). Interestingly increasing the donor strength leads to a slight decrease of the fluorescence quantum yield whereas increasing the acceptor strength leads to an increase (Table 1).

Figure 7

Two-photon absorption

The TPA spectra of the fluorophores were determined in the NIR range (700-1000 nm) by investigating their two-photon excited fluorescence (TPEF) in 10^{-4} M toluene solutions. The measurements were performed under excitation with 150 fs pulses from a Ti:sapphire laser,

using the experimental protocol of Xu and Webb.^[107] The quadratic dependence of the TPEF signal on the excitation intensity was checked for each data point, indicating that no photodegradation or saturation occurs. TPEF allows direct measurement of the TPEF action cross-section $\sigma_2\Phi$, the relevant figure of merit for imaging applications. From these values, the corresponding TPA cross-sections σ_2 can be derived. This method has been recognized as more reliable than nonlinear transmission measurements.^[108] We emphasize that experiments were conducted in the femtosecond regime, thus preventing contribution from linear non-resonant absorption or from excited-state absorption that is known to lead to artificially enhanced “effective” TPA cross-sections when measurements are conducted in the nanosecond regime. We also stress that the reported values are *non one-photon resonant* values, meaning that these chromophores could actually allow for the 3D resolution offered by selective two-photon excitation in the NIR region. This is not the case when even slight one-photon absorption is present (such as is the case in a number of chromophores with giant resonant TPA reported recently).^[109-112]

The TPA cross-sections were determined by comparing their TPEF to that of fluorescein in water (pH = 11),^[107] according to the following equation (1),

$$\sigma_s = \frac{S_s}{S_r} \frac{\eta_r}{\eta_s} \frac{\Phi_r}{\Phi_s} \frac{C_r}{C_s} \sigma_r \quad (1)$$

where the subscripts *s* and *r* refer to the sample and reference molecules, respectively. The intensity of signal collected by a photomultiplier was denoted as *S*. The η and Φ are the overall fluorescence collection efficiency and the fluorescence quantum yield, respectively. The number density of the molecules in solution is denoted as *C*. The σ_r is the TPA cross-section value of the reference (i.e. fluorescein). The experimental data are collected in Table 2.

From Table 2, we observe that in most cases the lowest energy TPA band is observed at lower wavelength than twice that of the lowest energy band in the one-photon absorption spectrum. In fact, as these quadrupoles are nearly centrosymmetric, the one-photon excited state has only little TPA activity^[41, 89, 90] and the two-photon allowed excited-state lies at higher energy. After two-photon excitation, relaxation to the lowest energy excited-state leads to the lowest energy one-photon allowed excited state thus allowing for radiative deactivation to take place. Note that given the spectral window investigated here, the TPA maxima corresponding to this higher-lying state is not systematically reached for all chromophores (Table 2).

Figure 8

End groups' effect

As noted from Table 2 and illustrated in Figure 8, push-push chromophores show larger TPA cross-sections in the NIR region than corresponding pull-pull derivatives, following the definite red shift of both the one-photon and two-photon absorption spectra and the reduction of the electronic gap between ground and excited-states. Increasing the strength of electron-donating end-groups results in a pronounced enhancement of the TPA cross-sections in the NIR region, again following the red-shift of both one and two-photon absorption spectra of push-push derivatives, as illustrated in Figure 9 and observed from Table 2. A similar effect is observed with electron-withdrawing groups (Figure 10).

Figure 9

Figure 10

Core effect

Comparison of push-push derivatives built from the different core moieties and bearing similar end-groups demonstrates that the nature of the conjugated core significantly influences the TPA spectra and governs the TPA cross-section magnitude. Independently of the connector nature, rigidification of the biphenyl unit, as obtained with fluorene, always leads to a significant increase of the TPA cross-section (Table 2). For instance, as observed from Figure 11, the push-push fluorene-cored derivative **24** shows higher TPA cross-sections than its biphenyl analogue **16a** in the whole red-NIR region.

Figure 11

Connector effect: phenylene-vinylene versus phenylene-ethynylene

We observe from Table 2 that replacement of a triple bond by a double bond always leads to a significant increase of the TPA cross-sections in the NIR region whatever the nature of the end-groups (D or A), of the core moiety and of the length of the conjugated rods. In addition, the replacement of triple bonds by double bonds also induces a significant broadening and red-shift of the TPA spectra as illustrated from Figure 12. This effect parallels the red-shift of

both absorption and emission bands, i.e. correlates with the reduction of the electronic gap between ground and excited states. As a result all fluorophores built from vinylene linkers instead of ethynylene linkers show much higher TPA cross-sections in the whole red-NIR region, the effect being more pronounced for higher wavelengths as clearly seen from Figure 12. This is of particular importance when imaging applications are concerned because (i) improved penetration depth is achieved when shifting to higher wavelength (due to reduction of scattering losses) and (ii) spectral broadening offers much more flexibility in terms of two-photon excitation (allowing for a wider choice of laser sources).

Figure 12

Connector effect: influence of arylene moieties

The nature of the arylene unit in the conjugated rods also plays an important role in tuning the TPA spectra and influencing the TPA cross-section magnitude. For derivatives of comparable length and bearing similar peripheral groups, we observe that replacement of the phenyl unit by a thienyl unit in the conjugated backbone has a markedly different impact depending on its position in the conjugated backbone. In particular, when a *terminal* phenyl ring is substituted by a thienyl ring, a major *decrease* of the TPA efficiency is obtained (Table 2). For instance compound **34a** displays TPA cross-sections about one order of magnitude lower than compound **24** (Figure 13a) all over the red-NIR range. A similar effect is observed when compounds **34b** and **31** are compared (Figure 13b). In contrast when the phenyl ring is replaced by a thienyl ring close to the core, a distinct increase of the TPA magnitude as well as a red-shift and *definite broadening of the TPA spectrum in the NIR region* is observed (Table 2). For instance compound **31** displays a TPA cross-section more than twice larger than that of compound **30** at 705 nm and more than three times larger at 900 nm. As a result fluorophore **31** maintains large *TPEF action cross-section* ($\sigma_2\Phi$) at 1 μm (i.e. 265 GM), a region of particular interest for imaging applications due to the increased penetration depth in tissues and availability of lower cost lasers. This effect parallels the bathochromic shift of both the absorption and emission bands, i.e. the significant reduction of the electronic gap.

We emphasize that the present study demonstrates that *the topology of the conjugated connectors dramatically influences the TPA properties*. Indeed replacing the phenyl ring by the less aromatic thienyl ring may have either a positive or negative effect on TPA properties depending on its location in the conjugated system. Furthermore *decreasing the aromaticity of*

the connector does not necessarily lead to enhanced TPA properties, even when the aromatic connector is located close to the core. This is clearly shown from comparison of compounds **17a** and **17b**: replacing the thienyl ring by a furyl ring – whose aromaticity is much lower^[113] – in the conjugated system results in a major *decrease* of the TPA cross-sections in the whole red-NIR spectral range (Figure 13c). This clearly demonstrates the limitations of the strategy consisting in reducing the aromaticity of conjugated systems for improvement of nonlinear, and particularly TPA, properties. A more subtle approach is clearly needed for molecular optimization of TPA properties.

Figure 13

Topology effect

The importance of the topology of the conjugated system is also clearly seen from the comparison of compounds **14** and **16b** that have the same end-groups, core and analogous connectors except for the location of the triple bond linker either close to the core (molecule **14**) or close to the end-groups (molecule **16b**). Although compounds **14** and **16b** have similar one-photon characteristics (Table 1), they clearly show *different* TPA spectra in the NIR range (Figure 14). Indeed when the triple bond linker is located closer to the core, the low energy TPA band is red-shifted, its maximum being shifted by 75 nm. Consequently compound **14** show higher TPA efficiency at wavelength longer than 770 nm. As an illustration the TPA cross-section of molecule **14** is more than twice larger than that of its analogue **16b** at 850 nm. Hence compound **14** while showing *similar* linear transparency than compound **16b** has broader TPA in the NIR. Such effect is of particular interest for optical limiting applications for which improved nonlinearity/transparency trade-off is an important issue. In that respect it is also interesting to note that chromophore **14** has lower fluorescence quantum yield while maintaining similar excited-state lifetime, thus offering better characteristics for broadband optical limiting in the visible-NIR region based on multiphoton absorption (including two-photon induced excited-state absorption in the nanosecond regime).^[35] This shows that subtle changes in the structures of the conjugated arms may have important implications in terms of molecular engineering for specific applications.

Figure 14

Length effect

The lengthening of the conjugated rods based on either phenylene-vinylene (Figure 15a) and thienylene-vinylene (Figure 15b) oligomers leads to a major increase of the TPA magnitude in the whole red-NIR range which parallels the lowering of the electronic gap between the ground and the first excited states (Table 2). It should be stressed that the TPA magnitude increases faster than the size of the molecule in the case of oligomeric phenylene-vinylene or thienylene-vinylene connectors as indicated by σ_2/N_e , the peak TPA cross-section normalized by the effective number of electrons^[114] (Table 2). In addition, we observe a marked red-shift of the TPA bands which results in a significant improvement of the TPA properties at higher wavelength. As a result elongated fluorophores show not only higher TPA peak but also much broader TPA activity in the target spectral range. This superlinear increase indicates that the lengthening approach is a valid strategy for TPA enhancement in the red-NIR range.

However, it should be stressed that the amplitude of the increase is markedly depending on the nature of the extensor. For instance, the lengthening of the conjugated rods based on phenylene-ethynylene oligomers does not necessarily lead to an increase of the TPA response (Table 2 and Figure 15c): a marked red shift and broadening of the TPA response is obtained in the red-NIR range (Figure 15c) whereas the one-photon absorption band is only slightly red-shifted (Figure 5c). Consequently, a major increase of the TPA efficiency in the NIR region is observed (by a factor of 3 to more than 10 in the 750-850 nm region) with nearly no loss of linear transparency. Hence phenylene-ethynylene oligomers appear as suitable connectors for broadband optical limiting in the visible-NIR region.

Figure 15

Finally, incorporation of a fluorenylene-vinylene or a thienylene-vinylene extensor in the conjugated arms also leads to major increase of the TPA efficiency in the whole red-NIR range, i.e. the spectral range of interest (Figure 16). Interestingly the strongest effect (both net increase and spectral broadening further to the NIR region) is obtained for the thienylene-vinylene connector, in correlation with the smallest energy gap between relaxed ground and excited states. As compared to insertion of a phenylene-vinylene, the insertion of a fluorenylene-vinylene allows major TPA increase mainly to the blue of the lowest-energy TPA peak. In contrast insertion of a thienylene-vinylene unit allows larger TPA increase in

the whole red-NIR range than insertion of a phenylene-vinylene unit (Figure 16). In comparison to both thienylene-vinylene oligomers and phenylene-vinylene oligomers, extended arms based upon the *alternation* of thienylene-vinylene and phenylene-vinylene moieties lead to major TPA enhancement and broadening in the red-NIR range. Indeed chromophore **31** shows a normalized TPA cross-section (σ_2/N_e) measured in the femtosecond regime similar to that of the best (in terms of *non one-photon resonant* TPA) chromophore reported up to now^[115] while being blue-shifted by nearly 40 nm. This molecule is thus particularly promising for optical limiting in the 700-900 nm region in the nanosecond regime. The present study thus provides evidence that by playing not only on the length of the conjugated arms but even more importantly on its nature and its topology, major (and nonlinear) increase in the TPA efficiency in the whole NIR range can be achieved.

Figure 16

Conclusion

This systematic study on the absorption, photoluminescence and two-photon absorption properties on such a broad series of quadrupolar fluorophores allowed us to derive structure-property relationships of great significance for both spectral tuning and amplification of the molecular TPA in the NIR spectral range. The influence of each moiety constituting these quadrupolar structures (cores, linkers, connectors and end-groups) has been studied in detail. Push-push systems were found to be more efficient than pull-pull systems and planarization of the core (fluorene vs biphenyl) always leads to an increase of the TPA cross-sections. The role of the conjugated rods should also be emphasized: their length is of course an important parameter, but the nature of the linkers (double or triple bonds) and of the arylene units (phenylene, thienylene, furylene, fluorenylene) is of particular importance as well. Concerning this last point, we have shown that the classical strategy consisting in reducing the aromaticity of the connectors does not necessarily give rise to an enhancement of the TPA response in the spectral region of interest. Moreover, we have demonstrated that the topology of the conjugated system, i.e. the location of linkers and connectors in the conjugated rods, can dramatically influence the TPA properties. Small changes in the structures may have important implications in terms of molecular engineering for specific applications, since the TPA properties (in terms of cross-sections, position of the maximum and bandwidth), as well

as the one-photon and the photoluminescence characteristics can be considerably affected. It becomes thus possible to optimize the transparency/TPA efficiency and the fluorescence/TPA efficiency trade-offs. With these findings in hands, quadrupolar fluorophores combining very large peak TPA cross-sections (up to 5480 GM), broad TPA bands in the whole 700-1000 nm range, and high fluorescence quantum yields (ranging from 0.45 to 0.98) could thus be obtained. Such compounds are of particular interest for TPEF microscopy^[45] as well as optical limiting in the visible^[39] and NIR^[35] regions.

Experimental Section

Photophysical methods.

UV/VIS spectra were recorded on a Jasco V-570 spectrophotometer.

Steady-state fluorescence measurements were performed at rt on dilute solutions (ca. 10^{-6} M) using an Edinburgh Instruments (FLS 920) spectrometer working in photon-counting mode, equipped with a calibrated quantum counter for excitation correction. Fully corrected emission spectra were obtained, for each compound, at $\lambda_{\text{ex}} = \lambda_{\text{max}}^{\text{abs}}$ with $A_{\text{ex}} \leq 0.1$ to minimize internal absorption. Fluorescence quantum yields were measured using standard methods^[116] on air-equilibrated samples at rt. Fluorescein in 0.1 M NaOH ($\Phi = 0.90$ at $\lambda_{\text{ex}} = 470$ nm) was used as a reference.^[117] The reported fluorescence quantum yields are within $\pm 10\%$.

Fluorescence lifetimes were measured by time-correlated single photon counting (TCSPC) using the same FLS 920 fluorimeter. Excitation was achieved by a hydrogen-filled nanosecond flashlamp (repetition rate 40 kHz). The instrument response (FWHM ca. 1 ns) was determined by measuring the light scattered by a Ludox suspension. The TCSPC traces were analyzed by standard iterative reconvolution methods implemented in the software of the fluorimeter. All compounds displayed strictly monoexponential fluorescence decays ($\chi^2 < 1.1$).

TPA (two-photon absorption) measurements were conducted by investigating the TPEF (two-photon excited fluorescence) of the fluorophores in toluene at rt on air-equilibrated solutions (10^{-4} M), using a Ti-sapphire laser delivering 150 fs excitation pulses, according to the experimental protocol established by Xu and Webb.^[107] This experimental protocol allows avoiding contributions from excited-state absorption that are known to result in largely overestimated TPA cross-sections. The quadratic dependence of the fluorescence intensity on the excitation intensity was verified for each data point, indicating that the measurements were carried out in intensity regimes in which saturation or photodegradation do not occur. TPEF measurements were calibrated relative to the absolute TPEF action cross-sections determined by Xu and Webb for fluorescein (10^{-4} M in 0.01 M aqueous NaOH) in the 690-1000 nm range.^[107, 118] This procedure provides the TPEF action cross-section $\sigma_2\Phi$ from which the corresponding σ_2 value is derived. The experimental uncertainty on the absolute action cross-sections determined by this method has been estimated to be $\pm 20\%$.^[107]

Synthetic Procedures.

General Methods: All air- or water-sensitive reactions were carried out under argon. Solvents were generally dried and distilled prior to use. Reactions were monitored by thin-layer chromatography on Merck silica gel or neutral aluminum oxide 60 F₂₅₄ precoated aluminum sheets. Column chromatography: Merck silica gel Si 60 (40-63 μm, 230-400 mesh), except otherwise noted. Melting points were determined on an Electrothermal IA9300 digital melting point instrument. NMR: Bruker AM 200 (¹H: 200.13 MHz), AM250 (¹H: 250.13 MHz, ¹³C: 62.90 MHz, ³¹P: 101.25 MHz), ARX 200 (¹H: 200.13 MHz, ¹³C: 50.32 MHz) or Avance AV 300 (¹H: 300.13 MHz, ¹³C: 75.48 MHz, ¹⁹F: 282.38 MHz, ³¹P: 121.50 MHz), in CDCl₃ solutions; ¹H chemical shifts (δ) are given in ppm relative to TMS as internal standard, *J* values in Hz, ¹³C chemical shifts relative to the central peak of CDCl₃ at 77.0 ppm, ³¹P relative to H₃PO₄ as external standard and ¹⁹F relative to CFCI₃ as internal standard. High and low resolution mass spectra measurements were performed at the Centre Régional de Mesures Physiques de l'Ouest (C.R.M.P.O., Rennes), using a Micromass MS/MS ZABSpec TOF instrument with EBE TOF geometry; LSIMS (Liquid Secondary Ion Mass Spectrometry) at 8 kV with Cs⁺ in *m*-nitrobenzyl alcohol (mNBA) or *o*-nitrophenyloctyl ether (oNPOE); ES⁺ (electrospray ionization, positive mode) at 4 kV; EI (Electron Ionization) at 70 eV; CI (Chemical Ionization) with NH₃ or CH₄ as ionization gas. Elemental analyses were performed at I.C.S.N. – C.N.R.S. (Gif-sur-Yvette, France) or at the C.R.M.P.O. Compounds **1b**,^[92] **1e**,^[93] **3a-c**,^[94] **5a**,^[95] **5b**,^[96] **7a**,^[97] **9a**,^[98] **12**^[100] and **15a**^[101] were synthesized according to the respective literature procedures. [(4-Methoxyphenyl)methyl]triphenylphosphonium bromide was prepared according to lit.^[119] [[5-(1-Piperidinyl)-2-thienyl]methyl]triphenylphosphonium iodide was prepared analogously to lit.^[94] Phosphonates **9b** and **11** were prepared analogously to lit.^[98] and lit.,^[120] respectively. 9,9-Dinonyl-9*H*-fluorene (**18a**) was prepared by reaction of fluorene with 1-bromononane using *n*-butyllithium in THF, analogously to lit.^[121]

4-[4-(Dihexylamino)phenyl]-2-methyl-3-butyn-2-ol (1c): Air was removed from a solution of *N,N*-dihexyl-4-iodobenzenamine (**1b**)^[92] (0.775 g, 2 mmol) in Et₃N (10 mL) by blowing argon for 20 min. Then CuI (15 mg, 0.08 mmol), Pd(PPh₃)₂Cl₂ (28 mg, 0.04 mmol) and 2-methyl-3-butyn-2-ol (0.254 mL, 2.6 mmol) were added, and the mixture was stirred at 40 °C for 12 h. After evaporation of the solvent, the residue was purified by column chromatography (CH₂Cl₂) to yield 0.566 g (82%) of **1c**; ¹H NMR (200.13 MHz, CDCl₃) δ 7.24 and 6.52 (AA'XX', *J*_{AX} = 9.0, 4H), 3.25 (m, 4H), 2.12 (s, 1H), 1.60 (s, 6H), 1.75-1.49 (m, 4H), 1.32 (m, 12H), 0.90 (t, *J* = 6.5, 6H); ¹³C NMR (50.32 MHz, CDCl₃) δ 147.9, 132.8,

111.1, 108.1, 91.2, 83.1, 65.7, 50.9, 31.7, 31.6, 27.1, 26.7, 22.6, 14.0; HRMS (EI) calcd for $C_{23}H_{37}NO$ (M^+) m/z 343.2875, found 343.2879; elemental analysis calcd (%) for $C_{23}H_{37}NO$ (343.55): C 80.41, H 10.85, N 4.08; found: C 80.14, H 10.61, N 3.95.

4-Ethynyl-*N,N*-dihexylbenzenamine (1d): To a solution of **1c** (0.457 g, 1.387 mmol) in 25 mL of toluene/*i*-PrOH (4/1), was added solid NaOH (0.14 g). The mixture was heated under reflux for 1 h. After cooling, the remaining NaOH was filtered off and the solvents were evaporated. The crude product was filtered through a pad of silica gel (CH_2Cl_2) to yield 0.330 g (87%) of **1d**; 1H NMR (200.13 MHz, $CDCl_3$) δ 7.32 and 6.52 (AA'XX', $J_{AX} = 9.0$, 4H), 3.25 (m, 4H), 2.95 (s, 1H), 1.65-1.47 (m, 4H), 1.32 (m, 12H), 0.89 (t, $J = 6.5$, 6H); ^{13}C NMR (50.32 MHz, $CDCl_3$) δ 148.2, 133.3, 111.0, 107.3, 85.1, 74.4, 50.9, 31.7, 27.1, 26.8, 22.7, 14.0; HRMS (EI) calcd for $C_{20}H_{31}N$ (M^+) m/z 285.2457, found 285.2465; elemental analysis calcd (%) for $C_{20}H_{31}N$ (285.47): C 84.15, H 10.94, N 4.91; found: C 84.04, H 10.77, N 4.71.

***N,N*-Dihexyl-4-[(4-iodophenyl)ethynyl]benzenamine (2a):** Air was removed from a solution of **1d** (0.162 g, 0.568 mmol) and 1,4-diiodobenzene (0.562 g, 1.702 mmol) in 6 mL of toluene/ Et_3N (5/1) by blowing argon for 20 min. Then CuI (2.2 mg, 0.012 mmol) and $Pd(PPh_3)_2Cl_2$ (8.1 mg, 0.012 mmol) were added, and the mixture was stirred at 30 °C for 6 h. After evaporation of the solvent, the crude product was purified by column chromatography (heptane/ CH_2Cl_2 , gradient from 100:0 to 90:10) to yield 0.197 g (71%) of **2a**; 1H NMR (200.13 MHz, $CDCl_3$) δ 7.64 and 7.21 (AA'XX', $J_{AX} = 8.5$, 4H), 7.34 and 6.56 (AA'XX', $J_{AX} = 9.0$, 4H), 3.27 (m, 4H), 1.67-1.46 (m, 4H), 1.31 (m, 12H), 0.90 (t, $J = 6.5$, 6H); ^{13}C NMR (50.32 MHz, $CDCl_3$) δ 148.0, 137.3, 132.9, 132.7, 123.9, 111.1, 108.1, 92.7, 92.5, 86.2, 50.9, 31.7, 27.1, 26.8, 22.7, 14.0; HRMS (LSIMS⁺, mNBA) calcd for $C_{26}H_{34}IN$ (M^+) m/z 487.1736, found 487.1738.

4-[[4-(Dihexylamino)phenyl]ethynyl]benzaldehyde (2b): Air was removed from a solution of **1d** (0.158 g, 0.553 mmol) and 4-bromobenzaldehyde (0.123 g, 0.664 mmol) in 6 mL of toluene/ Et_3N (5/1) by blowing argon for 20 min. Then CuI (2.1 mg, 0.011 mmol) and $Pd(PPh_3)_2Cl_2$ (7.8 mg, 0.011 mmol) were added, and the mixture was stirred at 40 °C for 15 h. After evaporation of the solvent, the crude product was purified by column chromatography (basic alumina, heptane/ CH_2Cl_2 , gradient from 100:0 to 60:40) to yield 0.160 g (74%) of **2b**; 1H NMR (200.13 MHz, $CDCl_3$) δ 9.98 (s, 1H), 7.82 and 7.60 (AA'XX', $J_{AX} = 8.4$, 4H), 7.38 and 6.57 (AA'XX', $J_{AX} = 9.0$, 4H), 3.28 (m, 4H), 1.71-1.48 (m, 4H), 1.32 (m, 12H), 0.90 (t, $J = 6.5$, 6H); ^{13}C NMR (50.32 MHz, $CDCl_3$) δ 191.4, 148.4, 134.5, 133.2, 131.4, 130.9, 129.5,

111.1, 107.6, 95.9, 86.9, 50.9, 31.7, 27.1, 26.7, 22.6, 14.0; HRMS (LSIMS⁺, mNBA) calcd for C₂₇H₃₅NO (M⁺) *m/z* 389.2719, found 389.2722; elemental analysis calcd (%) for C₂₇H₃₅NO (389.58): C 83.24, H 9.06, N 3.60; found: C 83.06, H 9.17, N 3.34.

4-[(1E)-2-(4-Iodophenyl)ethenyl]-N,N-dioctylbenzenamine (4a): To a solution of **3c**^[94] (8.826 g, 12.3 mmol) and 4-iodobenzaldehyde^[122] (2.85 g, 12.3 mmol) in anhyd CH₂Cl₂ (45 mL), was added *t*-BuOK (2.07 g, 18.4 mmol). The mixture was stirred at 20 °C for 5 h. After addition of water (60 mL), extraction with CH₂Cl₂, and drying (Na₂SO₄), the solvent was evaporated. The residue was purified by filtration through a short pad of silica gel (heptane/CH₂Cl₂ 50:50), to afford a mixture of isomers, which was dissolved in Et₂O (80 mL). A catalytic amount of I₂ was then added and the solution was stirred at 20 °C for 2 h under light exposure (75 W lamp). The organic layer was washed with aq Na₂S₂O₃ and dried (Na₂SO₄). After evaporation of the solvent, the crude product was purified by filtration through a pad of silica gel (CH₂Cl₂/heptane 90:10) to yield 5.696 g (85%) of **4a**: mp 50-51 °C; ¹H NMR (200.13 MHz, CDCl₃) δ 7.61 and 7.19 (AA'XX', *J*_{AX} = 8.4, 4H), 7.35 and 6.60 (AA'XX', *J*_{AX} = 8.9, 4H), 7.02 (d, *J* = 16.3, 1H), 6.76 (d, *J* = 16.3, 1H), 3.27 (m, 4H), 1.67-1.48 (m, 4H), 1.42-1.22 (m, 20H), 0.89 (t, *J* = 6.5, 6H); ¹³C NMR (50.32 MHz, CDCl₃) δ 147.9, 137.9, 137.5, 129.7, 127.9, 127.6, 123.9, 122.2, 111.5, 91.0, 51.0, 31.8, 29.5, 29.3, 27.3, 27.1, 22.6, 14.1; HRMS (LSIMS⁺, mNBA) calcd for C₃₀H₄₄IN (M⁺) *m/z* 545.2519, found 545.2518; elemental analysis calcd (%) for C₃₀H₄₄IN (545.59): C 66.04, H 8.13, N 2.57; found: C 66.09, H 8.28, N 2.46.

4-[(1E)-2-[4-(Dihexylamino)phenyl]ethenyl]benzaldehyde (4b): To a solution of **3b**^[94] (1.045 g, 1.57 mmol) and terephthalaldehyde mono-(diethylacetal) (0.329 g, 1.58 mmol) in anhyd CH₂Cl₂ (15 mL), was added *t*-BuOK (0.185 g, 1.65 mmol). The mixture was stirred at 20 °C for 24 h, then filtered through a short pad of silica gel. Evaporation of the solvents afforded the crude acetal, which was hydrolyzed at 20 °C for 1 h, using 10% HCl (25 mL) in THF (50 mL). Thereafter, THF was evaporated and CH₂Cl₂ was added. The two layers were separated and the organic layer was washed with aq NaHCO₃, dried (Na₂SO₄) and evaporated. The residue was dissolved in CH₂Cl₂, a catalytic amount of I₂ was added, and the solution was stirred at 20 °C for 3 h under light exposure (75 W lamp). The organic layer was washed with aq Na₂S₂O₃ and dried (Na₂SO₄). After evaporation of the solvent, the crude product was purified by column chromatography (cyclohexane/CH₂Cl₂ 20:80) to yield 0.517 g (84%) of **4b**,^[123] mp 72-73 °C; ¹H NMR (250.13 MHz, CDCl₃) δ 9.96 (s, 1H), 7.83 and 7.59 (AA'XX',

$J_{AX} = 8.2$ Hz, 4H), 7.41 and 6.63 (AA'XX', $J_{AX} = 8.8$ Hz, 4H), 7.20 (d, $J = 16.2$ Hz, 1H), 6.90 (d, $J = 16.2$ Hz, 1H), 3.29 (t, $J = 7.7$ Hz, 4H), 1.60 (m, 4H), 1.32 (m, 12H), 0.91 (t, $J = 6.5$ Hz, 6H); ^{13}C NMR (62.90 MHz, CDCl_3) δ 191.6, 148.5, 144.8, 134.4, 132.7, 130.3, 128.4, 126.1, 123.6, 121.9, 111.6, 51.1, 31.7, 27.3, 26.8, 22.7, 14.1; HRMS (CI, CH_4) calcd for $\text{C}_{27}\text{H}_{38}\text{NO}$ ($[\text{M}+\text{H}]^+$) m/z 392.2953, found 392.2951.

5-[(1E)-2-[4-(Diocetyl amino)phenyl]ethenyl]-2-furanecarboxaldehyde (6a): Reaction of **5a**^[95] (336 mg, 2 mmol) with **3c**^[94] (1.44 g, 2 mmol), as described for **4b**, for 15 h, with subsequent purification by column chromatography (heptane/ CH_2Cl_2 50:50), afforded 832 mg (95%) of **6a**; ^1H NMR (200.13 MHz, CDCl_3) δ 9.51 (s, 1H), 7.37 and 6.60 (AA'XX', $J_{AX} = 8.9$, 4H), 7.32 (d, $J = 16.1$, 1H), 7.23 (d, $J = 3.7$, 1H), 6.68 (d, $J = 16.1$, 1H), 6.41 (d, $J = 3.7$, 1H), 3.29 (m, 4H), 1.59 (m, 4H), 1.30 (m, 20H), 0.89 (t, $J = 6.5$, 6H); ^{13}C NMR (75.48 MHz, CDCl_3) δ 176.2, 160.5, 151.1, 148.7, 134.2, 130.5, 128.7, 122.7, 111.4, 109.5, 108.7, 51.0, 31.8, 29.5, 29.3, 27.3, 27.1, 22.6, 14.1.

5-[(1E)-2-[4-(Diocetyl amino)phenyl]ethenyl]-2-thiophenecarboxaldehyde (6b): Reaction of **5b**^[96] (366 mg, 1.99 mmol) with **3c**^[94] (1.56 g, 2.17 mmol), as described for **4b**, for 14 h, with subsequent purification by column chromatography (heptane/ CH_2Cl_2 50:50), afforded 715 mg (79%) of **6b**; ^1H NMR (200.13 MHz, CDCl_3) δ 9.81 (s, 1H), 7.62 (d, $J = 4.1$, 1H), 7.36 and 6.60 (AA'XX', $J_{AX} = 8.5$, 4H), 7.09 (d, $J = 16.3$, 1H), 7.04 (d, $J = 4.1$, 1H), 6.95 (d, $J = 16.3$, 1H), 3.29 (m, 4H), 1.56 (m, 4H), 1.30 (m, 20H), 0.89 (t, $J = 6.3$, 6H); ^{13}C NMR (50.32 MHz, CDCl_3) δ 182.3, 154.6, 148.7, 139.9, 137.6, 133.7, 128.6, 124.7, 122.7, 115.4, 111.5, 51.0, 31.8, 29.5, 29.3, 27.3, 27.1, 22.6, 14.1; HRMS (LSIMS⁺, mNBA) calcd for $\text{C}_{29}\text{H}_{43}\text{NOS}$ (M^+) m/z 453.3065, found 453.3068; elemental analysis calcd (%) for $\text{C}_{29}\text{H}_{43}\text{NOS}$ (453.72): C 76.77, H 9.55, N 3.09; found: C 76.78, H 9.49, N 2.96.

5-[(1E)-2-[4-(Dihexyl amino)phenyl]ethenyl]-2-thiophenecarboxaldehyde (6c): Reaction of **5b**^[96] (368 mg, 2 mmol) with **3b**^[94] (1.425 g, 2.15 mmol), as described for **4b**, for 14 h, with subsequent purification by column chromatography (heptane/ CH_2Cl_2 50:50), afforded 677 mg (85%) of **6c**; ^1H NMR (200.13 MHz, CDCl_3) δ 9.80 (s, 1H), 7.62 (d, $J = 4.3$, 1H), 7.36 and 6.60 (AA'XX', $J_{AX} = 8.8$, 4H), 7.09 (d, $J = 16.2$, 1H), 7.03 (d, $J = 4.3$, 1H), 6.95 (d, $J = 16.2$, 1H), 3.29 (m, 4H), 1.60 (m, 4H), 1.32 (m, 12H), 0.90 (t, $J = 6.3$, 6H); ^{13}C NMR (50.32 MHz, CDCl_3) δ 182.3, 154.6, 148.7, 139.9, 137.6, 133.7, 128.6, 124.7, 122.7, 115.4, 111.5, 51.0, 31.7, 27.2, 26.8, 22.7, 14.0; HRMS (LSIMS⁺, mNBA) calcd for $\text{C}_{25}\text{H}_{35}\text{NOS}$ (M^+) m/z

397.2439, found 397.2435; elemental analysis calcd (%) for C₂₅H₃₅NOS (397.62): C 75.52, H 8.87, N 3.52; found: C 75.64, H 9.06, N 3.28.

1-Bromo-4-(octylsulfonyl)benzene (8a): To a solution of 1-bromo-4-(octylthio)benzene (**7a**)^[97] (700 mg, 2.32 mmol) and Na₂WO₄·2H₂O (12 mg, 0.036 mmol) in 7.5 mL of EtOH/water (5:1), was slowly added, at 40 °C, 35% aq H₂O₂ (0.4 mL). Then, the mixture was heated at 80 °C and H₂O₂ (0.4 mL) was again slowly added. The mixture was refluxed for 1 h. After evaporation of the solvent, the residue was dissolved in CH₂Cl₂, washed with 10% Na₂CO₃, water and dried (Na₂SO₄). The solvent was removed to yield 720 mg (93%) of **8a**: mp 38-39 °C; ¹H NMR (200.13 MHz, CDCl₃) δ 7.78 and 7.71 (AA'XX', J_{AX} = 8.8, 4H), 3.07 (m, 2H), 1.69 (m, 2H), 1.24 (m, 10H), 0.86 (t, J = 6.5, 3H); ¹³C NMR (50.32 MHz, CDCl₃) δ 138.2, 132.6, 129.6, 128.9, 56.3, 31.6, 28.92, 28.86, 28.2, 22.6, 22.5, 14.0; HRMS (EI) calcd for C₁₄H₂₁⁷⁹BrO₂S (M⁺) m/z 332.0446, found 332.0418.

1-Bromo-4-[(trifluoromethyl)sulfonyl]benzene (8b): A solution of 1-bromo-4-[(trifluoromethyl)thio]benzene (**7b**) (922 mg, 3.59 mmol) in 35% aq H₂O₂ (12 mL) and glacial acetic acid (36 mL) was refluxed for 3 h. After addition of CH₂Cl₂, the organic layer was washed with NaHCO₃, then with water and dried (Na₂SO₄). The solvent was evaporated and the crude product was purified by column chromatography (heptane/CH₂Cl₂ 70:30) to yield 912 mg (89%) of **8b**: mp 63 °C (lit.^[124] mp 59.5-61.5 °C); ¹H NMR (200.13 MHz, CDCl₃) δ 7.91 and 7.83 (AA'XX', J_{AX} = 8.9, 4H); ¹³C NMR (50.32 MHz, CDCl₃) δ 133.4, 132.8, 132.0, 130.2, 119.6 (q, J = 325.8); HRMS (EI) calcd for C₇H₄⁷⁹BrF₃O₂S (M⁺) m/z 287.9067, found 287.9066.

Trimethyl[[4-[(trifluoromethyl)sulfonyl]phenyl]ethynyl]silane (8c): Air was removed from a solution of **8b** (390.0 mg, 1.35 mmol) in 5 mL of Et₃N by blowing argon for 20 min. Then CuI (5.1 mg, 27.0 μmol), Pd(PPh₃)₂Cl₂ (18.9 mg, 27.0 μmol), and trimethylsilylacetylene (288 μL, 2.02 mmol) were added under deaeration. Thereafter, the mixture was stirred at 40 °C for 3 h. The solvent was removed and the residue was purified by column chromatography (heptane/CH₂Cl₂ 75:25) to yield 364.0 mg (88%) of **8c**; ¹H NMR (200.13 MHz, CDCl₃) δ 7.94 and 7.68 (AA'XX', J_{AX} = 8.6, 4H), 0.25 (s, 9H); ¹³C NMR (50.32 MHz, CDCl₃) δ 132.9, 132.0, 130.5, 130.2, 119.7 (q, J = 325.8), 102.2, 101.9, -0.6.

1-Ethynyl-4-[(trifluoromethyl)sulfonyl]benzene (8d): To a solution of **8c** (356.6 mg, 1.16 mmol) in 3 mL of THF, was added TBAF (1 M in THF, 1.16 mL, 1.16 mmol) and the mixture was stirred for 2 min at 20 °C. After addition of CaCl₂, the solvent was removed and the

mixture was purified by column chromatography (heptane/CH₂Cl₂ 75:25) to yield 175.2 mg (64%) of **8d**; ¹H NMR (200.13 MHz, CDCl₃) δ 8.02 and 7.76 (AA'XX', J_{AX} = 8.4, 4H), 3.45 (s, 1H); ¹³C NMR (50.32 MHz, CDCl₃) δ 133.2, 131.0, 130.8, 130.6, 119.7 (q, J = 325.9), 83.4, 81.2; elemental analysis calcd (%) for C₉H₅F₃O₂S (234.20): C 46.16, H 2.15, S 13.69; found: C 45.88, H 2.09, S 13.66.

1-Iodo-4-[(1E)-2-[4-(octylsulfonyl)phenyl]ethenyl]benzene (10): To a solution of **9b** (1.702 g, 4.208 mmol) and 4-iodobenzaldehyde (1.057 g, 4.556 mmol) in anhyd THF (16 mL), was added NaH (273 mg, 60% dispersion in mineral oil). The mixture was stirred at 20 °C for 15 h. After addition of water, the product was extracted with CH₂Cl₂ and was then purified by column chromatography (heptane/CH₂Cl₂ 30:70) to yield 1.242 g (61%) of **10**: mp 158-159 °C; ¹H NMR (200.13 MHz, CDCl₃) δ 7.88 and 7.66 (AA'XX', J_{AX} = 8.5, 4H), 7.72 and 7.27 (AA'XX', J_{AX} = 8.5, 4H), 7.15 (s, 2H), 3.09 (m, 2H), 1.72 (m, 2H), 1.24 (m, 10H), 0.86 (t, J = 5.7, 3H); ¹³C NMR (50.32 MHz, CDCl₃) δ 142.1, 137.8, 137.6, 135.7, 131.2, 128.4, 127.2, 126.9, 94.0, 56.3, 31.5, 29.6, 28.84, 28.77, 22.6, 22.4, 14.0; HRMS (LSIMS⁺, mNBA) calcd for C₂₂H₂₈IO₂S ([M+H]⁺) m/z 483.0855, found 483.0864.

4,4'-[(1,1'-Biphenyl)-4,4'-diyldi-2,1-ethynediyl]bis(N,N-dihexylbenzenamine) (13a): Air was removed from a solution of **12**^[100] (90 mg, 0.445 mmol) and **1b**^[92] (431 mg, 1.112 mmol) in 4 mL of toluene/Et₃N (5/1) by blowing argon for 20 min. Then CuI (3.4 mg, 0.018 mmol) and Pd(PPh₃)₂Cl₂ (12.5 mg, 0.018 mmol) were added, and deaeration was continued for 10 min. Thereafter the mixture was stirred at 20 °C for 2 h. The solvent was removed under reduced pressure, and the crude product was purified by column chromatography (heptane/CH₂Cl₂ 90:10 then 80:20) to yield 270.4 mg (84%) of **13a**: mp 113.5-114.5 °C; ¹H NMR (200.13 MHz, CDCl₃) δ 7.56 (s, 8H), 7.38 and 6.58 (AA'XX', J_{AX} = 9.0, 8H), 3.28 (m, 8H), 1.66-1.52 (m, 8H), 1.32 (m, 24H), 0.91 (t, J = 6.5, 12H); ¹³C NMR (50.32 MHz, CDCl₃) δ 147.9, 139.2, 132.9, 131.6, 126.6, 123.4, 111.2, 108.6, 91.9, 87.0, 50.9, 31.7, 27.2, 26.8, 22.7, 14.0; HRMS (LSIMS⁺, mNBA) calcd for C₅₂H₆₈N₂ (M⁺) m/z 720.5383, found 720.5390; elemental analysis calcd (%) for C₅₂H₆₈N₂ (721.12): C 86.61, H 9.50, N 3.88; found: C 86.42, H 9.64, N 3.90.

4,4'-[(1,1'-Biphenyl)-4,4'-diyldi-2,1-ethynediyl-4,1-phenylene-2,1-ethynediyl]bis(N,N-dihexylbenzenamine) (13b): Reaction of **12** (26.1 mg, 0.129 mmol) with **2a** (146 mg, 0.299 mmol), as described for **13a**, with subsequent purification by column chromatography (heptane/CH₂Cl₂, gradient from 50:50 to 0:100) and crystallization, afforded 102.6 mg (86%)

of **13b**: mp 234–235 °C; ¹H NMR (300.13 MHz, CDCl₃) δ 7.61 (s, 8H), 7.49 and 7.46 (AA'XX', *J*_{AX} = 8.7, 8H), 7.36 and 6.56 (AA'XX', *J*_{AX} = 9.3, 8H), 3.27 (m, 8H), 1.66–1.52 (m, 8H), 1.31 (m, 24H), 0.90 (t, *J* = 6.6, 12H); ¹³C NMR (50.32 MHz, CDCl₃) δ 148.1, 140.0, 132.9, 132.1, 131.4, 131.1, 126.9, 124.3, 122.5, 121.8, 111.1, 108.3, 93.2, 90.6, 90.4, 87.0, 50.9, 31.7, 27.2, 26.8, 22.7, 14.0; MS (ES⁺, CH₂Cl₂/MeOH) *m/z* 921.6 ([M+H]⁺), 461.4 ([M+2H]²⁺); HRMS (ES⁺, CH₂Cl₂/MeOH) calcd for C₆₈H₇₇N₂ ([M+H]⁺) *m/z* 921.6087, found 921.6110; elemental analysis calcd (%) for C₆₈H₇₆N₂ (921.36): C 88.65, H 8.31, N 3.04; found: C 88.72, H 8.41, N 2.80.

4,4'-[(1,1'-Biphenyl)-4,4'-diylbis[2,1-ethynediyl-4,1-phenylene-(1E)-2,1-

ethenediyl]]bis(*N,N*-dioctylbenzenamine) (14**):** Reaction of **12** (34.6 mg, 0.171 mmol) with **4a** (215 mg, 0.394 mmol), as described for **13a**, for 3.5 h, with subsequent purification by column chromatography (heptane/CH₂Cl₂, gradient from 40:60 to 0:100) and crystallization, afforded 144.4 mg (81%) of **14**: mp 221–222 °C; ¹H NMR (200.13 MHz, CDCl₃) δ 7.61 (s, 8H), 7.51 and 7.44 (AA'XX', *J*_{AX} = 8.8, 8H), 7.38 and 6.62 (AA'XX', *J*_{AX} = 8.8, 8H), 7.08 (d, *J* = 16.3, 2H), 6.86 (d, *J* = 16.3, 2H) 3.28 (m, 8H), 1.67–1.52 (m, 8H), 1.31 (m, 40H), 0.89 (t, *J* = 6.3, 12H); ¹³C NMR (50.32 MHz, CDCl₃) δ 148.0, 139.8, 138.5, 132.0, 131.8, 129.9, 128.8, 127.9, 126.8, 125.8, 124.1, 122.7, 120.8, 111.6, 90.9, 89.7, 51.1, 31.8, 29.5, 29.3, 27.3, 27.2, 22.6, 14.1; HRMS (LSIMS⁺, mNBA) calcd for C₇₆H₉₆N₂ (M⁺) *m/z* 1036.7574, found 1036.7565; elemental analysis calcd (%) for C₇₆H₉₆N₂ (1037.61): C 87.97, H 9.33, N 2.70; found: C 87.95, H 9.56, N 2.71.

[(1,1'-Biphenyl)-4,4'-diylbis(methylene)]bisphosphonic acid tetraethyl ester (15b**):** A solution of **15a**^[101] (10.20 g, 30.0 mmol) and P(OEt)₃ (13.34 g, 80 mmol) in toluene (60 mL) was refluxed for 60 h. Filtration of the precipitate obtained after cooling at 0 °C gave 11.7 g (86%) of **15b**: mp 109 °C (lit.^[125] mp 109–110 °C); ¹H NMR (200.13 MHz, CDCl₃) δ 7.45 (d, *J* = 8.0, 4H), 7.28 (dd, *J* = 8.0, 2.1, 4H), 3.96 (dq, *J* = 7.8, 7.1, 8H), 3.10 (d, *J* = 21.6, 4H), 1.18 (t, *J* = 7.0, 12H); ¹³C NMR (50.32 MHz, CDCl₃) δ 139.2, 130.7 (d, *J* = 9.2), 130.1 (d, *J* = 6.5), 127.1 (d, *J* = 2.3), 62.1 (d, *J* = 6.7), 33.4 (d, *J* = 137.3), 16.4 (d, *J* = 6.0); ³¹P NMR (101.25 MHz, CDCl₃) δ 26.20; HRMS (CI, CH₄) calcd for C₂₂H₃₃O₆P₂ [M + H]⁺ *m/z* 455.1752, found 455.1749.

4,4'-[(1,1'-Biphenyl)-4,4'-diyl-di-(1E)-2,1-ethenediyl]]bis(*N,N*-dihexylbenzenamine) (16a**):**

To a solution of **15b** (1.70 g, 3.74 mmol) and **1e**^[93] (2.494 g, 7.48 mmol) in anhyd THF (70 mL), was added NaH (0.45 g, 60% dispersion in mineral oil). The mixture was stirred at 20

°C for 20 h, then under reflux for 4 h. After addition of water (25 mL), the THF was evaporated. The resulting precipitate was filtered and washed successively with EtOH and pentane. The crude product was then purified by column chromatography (heptane/CH₂Cl₂ 60:40) to yield 1.90 g (70%) of **16a**: mp 147-148 °C; ¹H NMR (200.13 MHz, CDCl₃) δ 7.59 and 7.53 (AA'XX', *J*_{AX} = 8.6, 8H), 7.39 and 6.62 (AA'XX', *J*_{AX} = 8.8, 8H), 7.08 (d, *J* = 16.2, 2H), 6.90 (d, *J* = 16.2, 2H), 3.28 (m, 8H), 1.59 (m, 8H), 1.32 (m, 24H), 0.91 (t, *J* = 6.4, 12H); ¹³C NMR (50.32 MHz, CDCl₃) δ 147.8, 138.7, 137.2, 128.8, 127.8, 126.8, 126.3, 124.4, 123.1, 111.6, 51.0, 31.7, 27.3, 26.8, 22.7, 14.1; HRMS (LSIMS⁺, mNBA) calcd for C₅₂H₇₂N₂ (M⁺) *m/z* 724.5696, found 724.5694; elemental analysis calcd (%) for C₅₂H₇₂N₂ (725.15): C 86.13, H 10.01, N 3.86; found: C 85.81, H 10.03, N 3.78.

4,4'-[(1,1'-Biphenyl)-4,4'-diylbis[(1E)-2,1-ethenediyl-4,1-phenylene-2,1-

ethenediyl]]bis(*N,N*-dihexylbenzenamine) (16b**):** To a solution of **15b** (75.4 mg, 0.166 mmol), **2b** (148.5 mg, 0.381 mmol) and 18-crown-6 (4.3 mg) in anhyd THF (8 mL), was added NaH (26 mg, 60% dispersion in mineral oil). The mixture was stirred at 40 °C for 3 h. After addition of water, the precipitate was filtered and washed with water, EtOH, Et₂O and pentane successively, and dried under vacuum. The product was then purified by column chromatography (heptane/CH₂Cl₂, gradient from 40:60 to 0:100) to yield 128 mg (84%) of **16b**: mp 243-244 °C; ¹H NMR (200.13 MHz, CDCl₃) δ 7.65 and 7.59 (AA'XX', *J*_{AX} = 8.7, 8H), 7.49 (s, 8H), 7.37 and 6.57 (AA'XX', *J*_{AX} = 9.1, 8H), 7.15 (s, 4H), 3.28 (m, 8H), 1.65-1.50 (m, 8H), 1.32 (m, 24H), 0.91 (t, *J* = 6.6, 12H); MS (ES⁺, CHCl₃/MeOH) *m/z* 925.6 ([M+H]⁺), 463.4 ([M+2H]²⁺); HRMS (ES⁺, CHCl₃/MeOH) calcd for C₆₈H₈₁N₂ ([M+H]⁺) *m/z* 925.6400, found 925.6391; elemental analysis calcd (%) for C₆₈H₈₀N₂ (925.39): C 88.26, H 8.71, N 3.03; found: C 88.03, H 8.95, N 2.97.

4,4'-[(1,1'-Biphenyl)-4,4'-diylbis[(1E)-2,1-ethenediyl-5,2-furannediyl-(1E)-2,1-

ethenediyl]]bis(*N,N*-dioctylbenzenamine) (17a**):** To a solution of **15b** (216 mg, 0.475 mmol) and **6a** (422 mg, 0.965 mmol) in anhyd THF (10 mL), was added NaH (150 mg, 60% dispersion in mineral oil). The mixture was stirred at 20 °C for 19 h. After addition of water, the precipitate was filtered and washed with water, EtOH and pentane successively, and dried under vacuum, to yield 390 mg (80%) of **17a**: mp 247-249 °C; ¹H NMR (200.13 MHz, CDCl₃) δ 7.63 and 7.56 (AA'XX', *J*_{AX} = 8.3, 8H), 7.37 and 6.62 (AA'XX', *J*_{AX} = 8.6, 8H), 7.13 (d, *J* = 16.3, 2H), 7.08 (d, *J* = 15.8, 2H), 6.91 (d, *J* = 16.3, 2H), 6.67 (d, *J* = 15.8, 2H), 6.39 (d, *J* = 3.3, 2H), 6.28 (d, *J* = 3.3, 2H), 3.29 (m, 8H), 1.56 (m, 8H), 1.31 (m, 40H), 0.89 (t,

$J = 6.6$, 12H); ^{13}C NMR (50.32 MHz, CDCl_3) δ 154.3, 152.1, 147.8, 139.4, 136.4, 131.3, 129.4, 128.0, 127.7, 127.0, 126.7, 125.7, 124.1, 116.3, 111.6, 109.2, 51.0, 31.8, 29.5, 29.3, 27.3, 27.2, 22.7, 14.1; HRMS (LSIMS⁺, mNBA) calcd for $\text{C}_{72}\text{H}_{96}\text{N}_2\text{O}_2$ (M^+) m/z 1020.7472, found 1020.7477.

4,4'-[(1,1'-Biphenyl)-4,4'-diylbis[(1E)-2,1-ethenediyl-5,2-thiophenediyl-(1E)-2,1-ethenediyl]]bis(*N,N*-dihexylbenzenamine) (17b): Reaction of **15b** (227 mg, 0.5 mmol) with **6c** (415 mg, 1.04 mmol), as described for **17a**, for 16 h, afforded 301 mg (64%) of **17b**: mp 250-252 °C; ^1H NMR (200.13 MHz, CDCl_3) δ 7.62 and 7.53 (AA'XX', $J_{\text{AX}} = 8.3$, 8H), 7.33 and 6.61 (AA'XX', $J_{\text{AX}} = 8.7$, 8H), 7.23 (d, $J = 16.6$, 2H), 6.97 (d, $J = 16.0$, 2H), 6.94 (d, $J = 3.7$, 2H), 6.89 (d, $J = 16.6$, 2H), 6.86 (d, $J = 3.7$, 2H), 6.84 (d, $J = 16.0$, 2H), 3.28 (m, 8H), 1.57 (m, 8H), 1.32 (m, 24H), 0.91 (t, $J = 6.2$, 12H); HRMS (LSIMS⁺, mNBA) calcd for $\text{C}_{64}\text{H}_{80}\text{N}_2\text{S}_2$ (M^+) m/z 940.5763, found 940.5758.

2,7-Diiodo-9,9-dinonyl-9H-fluorene (18b): To a mixture of **18a** (10.0 g, 23.88 mmol), AcOH (25 mL), concd H_2SO_4 (0.75 mL) and water (5 mL) at 75 °C, were added H_5IO_6 (1.09 g) and I_2 (2.42 g). The solution was heated at 75 °C for 1 h, then AcOH (25 mL), H_5IO_6 (1.09 g) and I_2 (2.42 g) were again added and the heating was continued at 75 °C for 1 h. The reaction mixture was cooled, diluted with CH_2Cl_2 and a solution of $\text{Na}_2\text{S}_2\text{O}_3$ was added. The two layers were separated and the organic layer was washed with 1 N NaOH, then with water and dried (Na_2SO_4). After evaporation of the solvent, the residue was purified by column chromatography (heptane) to yield 11.02 g (69%) of **18b**; ^1H NMR (200.13 MHz, CDCl_3) δ 7.65 (d, $J = 8.5$, 2H), 7.40 (d, $J = 8.5$, 2H), 7.63 (s, 2H), 1.89 (m, 4H), 1.29-1.01 (m, 24H), 0.85 (t, $J = 6.7$, 6H), 0.57 (m, 4H); ^{13}C NMR (50.32 MHz, CDCl_3) δ 152.5, 139.7, 136.0, 132.0, 121.5, 93.1, 55.5, 40.0, 31.8, 29.8, 29.4, 29.2, 29.1, 23.6, 22.6, 14.1; HRMS (LSIMS⁺, mNBA) calcd for $\text{C}_{31}\text{H}_{44}\text{I}_2$ (M^+) m/z 670.1533, found 670.1527; elemental analysis calcd (%) for $\text{C}_{31}\text{H}_{44}\text{I}_2$ (670.50): C 55.53, H 6.61; found: C 55.74, H 6.89.

4,4'-(9,9-Dinonyl-9H-fluorene-2,7-diyl)bis(2-methyl-3-butyn-2-ol) (18c): Air was removed from a solution of **18b** (4.19 g, 6.25 mmol) in 20 mL of Et_3N by blowing argon for 20 min. Then CuI (48.1 mg, 0.253 mmol), $\text{Pd}(\text{PPh}_3)_2\text{Cl}_2$ (176.0 mg, 0.251 mmol) and 2-methyl-3-butyn-2-ol (1.868 mL, 19.12 mmol) were added, and the mixture was stirred at 20 °C for 16 h. The precipitate which separated was filtered off and washed with Et_2O . The filtrate was evaporated to dryness and the residue was purified by column chromatography (heptane/ CH_2Cl_2 30:70) to yield 2.64 g (72%) of **18c**; ^1H NMR (200.13 MHz, CDCl_3) δ 7.59

(d, $J = 8.5$, 2H), 7.39 (d, $J = 8.5$, 2H), 7.37 (s, 2H), 2.10 (s, 2H), 1.92 (m, 4H), 1.66 (s, 12H), 1.28-0.98 (m, 24H), 0.84 (t, $J = 6.7$, 6H), 0.54 (m, 4H); ^{13}C NMR (50.32 MHz, CDCl_3) δ 150.8, 140.4, 130.6, 125.9, 121.4, 119.7, 94.0, 82.9, 65.6, 55.0, 40.3, 31.7, 31.4, 29.9, 29.4, 29.2, 29.1, 23.6, 22.5, 14.0; MS (LSIMS⁺, mNBA) m/z 582.4 ($[\text{M}^{\cdot+}]$, 63), 565.4 ($[\text{M}+\text{H}^+-\text{H}_2\text{O}]$, 100); HRMS (LSIMS⁺, mNBA) calcd for $\text{C}_{41}\text{H}_{58}\text{O}_2$ ($\text{M}^{\cdot+}$) m/z 582.4437, found 582.4432.

2,7-Diethynyl-9,9-dinonyl-9H-fluorene (18d): To a refluxing solution of **18c** (1.72 g, 2.95 mmol) in 30 mL of toluene/*i*-PrOH (4/1), was added solid KOH (0.494 g, 8.8 mmol). The mixture was stirred under reflux for 0.5 h. After cooling, the mixture was filtered through Celite[®] and the filter cake was washed with CH_2Cl_2 . The combined filtrate and washings were dried (Na_2SO_4) and evaporated to give a crude product, which was purified by column chromatography (heptane) to yield 1.21 g (88%) of **18d**; ^1H NMR (200.13 MHz, CDCl_3) δ 7.63 (d, $J = 8.6$, 2H), 7.48 (d, $J = 8.6$, 2H), 7.46 (s, 2H), 3.14 (s, 2H), 1.93 (m, 4H), 1.27-0.99 (m, 24H), 0.84 (t, $J = 6.7$, 6H), 0.56 (m, 4H); ^{13}C NMR (50.32 MHz, CDCl_3) δ 151.0, 141.0, 131.2, 126.5, 120.8, 119.9, 84.5, 77.3, 55.2, 40.2, 31.8, 29.9, 29.5, 29.2, 29.1, 23.6, 22.6, 14.1; HRMS (LSIMS⁺, mNBA) calcd for $\text{C}_{35}\text{H}_{46}$ ($\text{M}^{\cdot+}$) m/z 466.3600, found 466.3602.

4,4'-[(9,9-Dinonyl-9H-fluorene-2,7-diyl)di-2,1-ethynediyl]bis(*N,N*-dihexylbenzenamine) (19a): Reaction of **18d** (231.6 mg, 0.496 mmol) with **1b**^[92] (462.9 mg, 1.195 mmol), as described for **13a**, for 3 h, with subsequent purification by column chromatography (heptane/ CH_2Cl_2 90:10), afforded 221 mg (45%) of **19a**; ^1H NMR (200.13 MHz, CDCl_3) δ 7.60 (d, $J = 8.3$, 2H), 7.46 (d, $J = 8.3$, 2H), 7.45 (s, 2H), 7.39 and 6.57 (AA'XX', $J_{\text{AX}} = 9.0$, 8H), 3.27 (m, 8H), 1.96 (m, 4H), 1.58 (m, 8H), 1.32 (m, 24H), 1.30-0.99 (m, 24H), 0.90 (t, $J = 6.6$, 12H), 0.83 (t, $J = 6.7$, 6H), 0.61 (m, 4H); ^{13}C NMR (50.32 MHz, CDCl_3) δ 150.9, 147.8, 140.0, 132.8, 130.3, 125.5, 122.7, 119.6, 111.2, 108.7, 91.1, 88.2, 55.1, 50.9, 40.5, 31.8, 31.7, 30.1, 29.6, 29.3, 29.2, 27.2, 26.8, 23.7, 22.7, 22.6, 14.1, 14.0; HRMS (LSIMS⁺, mNBA) calcd for $\text{C}_{71}\text{H}_{104}\text{N}_2$ ($\text{M}^{\cdot+}$) m/z 984.8200, found 984.8209; elemental analysis calcd (%) for $\text{C}_{71}\text{H}_{104}\text{N}_2$ (985.62): C 86.52, H 10.64, N 2.84; found: C 86.12, H 10.85, N 2.88.

4,4'-[(9,9-Dinonyl-9H-fluorene-2,7-diyl)bis(2,1-ethynediyl-4,1-phenylene-2,1-ethynediyl)]bis(*N,N*-dihexylbenzenamine) (19b): Reaction of **18d** (100 mg, 0.214 mmol) with **2a** (241 mg, 0.494 mmol), as described for **13a**, for 20 h, with subsequent purification by column chromatography (heptane/ CH_2Cl_2 , gradient from 90:10 to 80:20), afforded 208.6 mg (82%) of **19b**; ^1H NMR (200.13 MHz, CDCl_3) δ 7.67 (d, $J = 8.4$, 2H), 7.52 (d, $J = 8.4$, 2H),

7.52 and 7.47 (AA'XX', $J_{AX} = 8.8$, 8H), 7.50 (s, 2H), 7.37 and 6.57 (AA'XX', $J_{AX} = 8.9$, 8H), 3.28 (m, 8H), 1.98 (m, 4H), 1.58 (m, 8H), 1.32 (m, 24H), 1.30-1.02 (m, 24H), 0.91 (t, $J = 6.5$, 12H), 0.82 (t, $J = 6.6$, 6H), 0.61 (m, 4H); ^{13}C NMR (50.32 MHz, CDCl_3) δ 151.1, 148.0, 140.7, 132.9, 131.4, 131.1, 130.7, 125.9, 124.2, 122.0, 121.9, 120.0, 111.1, 108.4, 93.1, 91.9, 89.8, 87.0, 55.2, 50.9, 40.3, 31.8, 31.7, 30.0, 29.5, 29.3, 29.2, 27.2, 26.8, 23.7, 22.7, 22.6, 14.04, 14.02; HRMS (LSIMS⁺, oNPOE) calcd for $\text{C}_{87}\text{H}_{112}\text{N}_2$ ($\text{M}^{\cdot+}$) m/z 1184.8826, found 1184.8813; elemental analysis calcd (%) for $\text{C}_{87}\text{H}_{112}\text{N}_2$ (1185.86): C 88.12, H 9.52, N 2.36; found: C 88.00, H 9.65, N 2.18.

4,4'-[(9,9-Dinonyl-9H-fluorene-2,7-diyl)bis[2,1-ethynediyl-4,1-phenylene-(1E)-2,1-ethenediyl]]bis(N,N-dioctylbenzenamine) (20): Reaction of **18d** (96 mg, 0.206 mmol) with **4a** (272 mg, 0.498 mmol), as described for **13a**, for 15 h, with subsequent purification by column chromatography (heptane/ CH_2Cl_2 , gradient from 90:10 to 80:20), afforded 223 mg (83%) of **20**; ^1H NMR (200.13 MHz, CDCl_3) δ 7.66 (d, $J = 8.6$, 2H), 7.52 (d, $J = 8.6$, 2H), 7.52 and 7.45 (AA'XX', $J_{AX} = 8.6$, 8H), 7.50 (s, 2H), 7.38 and 6.62 (AA'XX', $J_{AX} = 8.7$, 8H), 7.08 (d, $J = 16.1$, 2H), 6.86 (d, $J = 16.1$, 2H), 3.28 (m, 8H), 1.98 (m, 4H), 1.59 (m, 8H), 1.31 (m, 40H), 1.30-1.02 (m, 24H), 0.89 (t, $J = 6.2$, 12H), 0.83 (t, $J = 6.7$, 6H), 0.62 (m, 4H); ^{13}C NMR (50.32 MHz, CDCl_3) δ 151.1, 148.0, 140.6, 138.4, 131.8, 130.7, 129.9, 127.9, 125.8, 125.7, 124.2, 122.8, 122.1, 121.0, 119.9, 111.6, 90.9, 90.3, 55.2, 51.0, 40.4, 31.82, 31.80, 30.0, 29.52, 29.48, 29.31, 29.3, 29.2, 27.3, 27.2, 23.7, 22.64, 22.61, 14.1, 14.0; HRMS (LSIMS⁺, oNPOE) calcd for $\text{C}_{95}\text{H}_{132}\text{N}_2$ ($\text{M}^{\cdot+}$) m/z 1301.0391, found 1301.0381; elemental analysis calcd (%) for $\text{C}_{95}\text{H}_{132}\text{N}_2$ (1302.10): C 87.63, H 10.22, N 2.15; found: C 87.48, H 10.13, N 1.91.

9,9-Dinonyl-2,7-bis[[4-(octylsulfonyl)phenyl]ethynyl]-9H-fluorene (21a): Reaction of **18d** (106.7 mg, 0.229 mmol) with **8a** (174 mg, 0.523 mmol), as described for **13a**, at 45 °C for 6 h, with subsequent purification by column chromatography (heptane/ CH_2Cl_2 35:65), afforded 186.0 mg (84%) of **21a**; ^1H NMR (200.13 MHz, CDCl_3) δ 7.91 and 7.73 (AA'XX', $J_{AX} = 8.6$, 8H), 7.72 (d, $J = 8.0$, 2H), 7.56 (d, $J = 8.0$, 2H), 7.54 (s, 2H), 3.11 (m, 4H), 2.00 (m, 4H), 1.73 (m, 4H), 1.41-1.02 (m, 44H), 0.87 (t, $J = 6.5$, 6H), 0.81 (t, $J = 6.6$, 6H), 0.61 (m, 4H); ^{13}C NMR (50.32 MHz, CDCl_3) δ 151.2, 141.2, 138.1, 132.0, 131.0, 129.1, 128.1, 126.1, 121.1, 120.2, 94.3, 88.2, 56.3, 55.3, 40.2, 31.7, 31.6, 29.9, 29.4, 29.2, 29.1, 28.9, 28.8, 28.2, 23.7, 22.59, 22.55, 22.50, 14.02, 14.01; HRMS (LSIMS⁺, mNBA) calcd for $\text{C}_{63}\text{H}_{86}\text{O}_4\text{S}_2$ ($\text{M}^{\cdot+}$) m/z

970.5968, found 970.5981; elemental analysis calcd (%) for C₆₃H₈₆O₄S₂ (971.49): C 77.89, H 8.92; found: C 77.66, H 8.96.

9,9-Dinonyl-2,7-bis[[4-[(trifluoromethyl)sulfonyl]phenyl]ethynyl]-9H-fluorene (21b):

Reaction of **18b** (175.7 mg, 0.26 mmol) with **8d** (153.4 mg, 0.66 mmol), as described for **13a**, at 40 °C for 14 h, with subsequent purification by column chromatography (heptane/CH₂Cl₂ 80:20), afforded 138.0 mg (60%) of **21b**; ¹H NMR (200.13 MHz, CDCl₃) δ 8.04 and 7.82 (AA'XX', J_{AX} = 8.5, 8H), 7.74 (d, J = 7.9, 2H), 7.58 (d, J = 7.9, 2H), 7.56 (s, 2H), 2.02 (m, 4H), 1.26-1.07 (m, 24H), 0.81 (t, J = 6.6, 6H), 0.62 (m, 4H); ¹³C NMR (75.48 MHz, CDCl₃) δ 151.4, 141.6, 132.5, 132.4, 131.3, 130.7, 129.9, 126.4, 120.9, 120.4, 120.2 (q, J = 325.9), 96.7, 87.8, 55.5, 40.2, 31.8, 29.9, 29.5, 29.2, 23.7, 22.6, 14.0; ¹⁹F NMR (282.38 MHz, CDCl₃) δ -78.22; HRMS (LSIMS⁺, mNBA) calcd for C₄₉H₅₂F₆O₄S₂ (M⁺) m/z 882.3211, found 882.3225.

9,9-Dinonyl-2,7-bis[[4-[(1E)-2-[4-(octylsulfonyl)phenyl]ethenyl]phenyl]ethynyl]-9H-

fluorene (21c): Reaction of **18d** (109.7 mg, 0.235 mmol) with **10** (271 mg, 0.562 mmol), as described for **13a**, at 35 °C for 14 h, with subsequent purification by column chromatography (heptane/CH₂Cl₂ 25:75 then 20:80), afforded 239.8 mg (87%) of **21c**: mp 164-165 °C; ¹H NMR (200.13 MHz, CDCl₃) δ 7.89 and 7.68 (AA'XX', J_{AX} = 8.6, 8H), 7.69 (d, J = 8.0, 2H), 7.53 (d, J = 8.0, 2H), 7.60 and 7.54 (AA'XX', J_{AX} = 8.8, 8H), 7.54 (s, 2H), 7.27 (d, J = 16.5, 2H), 7.16 (d, J = 16.5, 2H), 3.10 (m, 4H), 2.01 (m, 4H), 1.73 (m, 4H), 1.41-1.00 (m, 44H), 0.86 (t, J = 6.4, 6H), 0.83 (t, J = 6.7, 6H), 0.62 (m, 4H); ¹³C NMR (50.32 MHz, CDCl₃) δ 151.1, 142.3, 140.7, 137.6, 136.1, 131.9, 131.7, 130.8, 128.5, 127.3, 127.0, 126.8, 125.9, 123.3, 121.8, 120.0, 92.0, 89.8, 56.3, 55.2, 40.3, 31.7, 31.6, 29.9, 29.4, 29.2, 29.1, 28.9, 28.8, 28.2, 23.7, 22.6, 22.54, 22.48, 14.01, 13.98; HRMS (LSIMS⁺, mNBA) calcd for C₇₉H₉₈O₄S₂ (M⁺) m/z 1174.6907, found 1174.6913; elemental analysis calcd (%) for C₇₉H₉₈O₄S₂ (1175.76): C 80.70, H 8.40; found: C 80.71, H 8.41.

2,7-Dibromo-9,9-dinonyl-9H-fluorene (22a): To 300 mL of a CH₂Cl₂ solution of **18a** (18 g, 43 mmol) and iodine (22 mg, 0.087 mmol), was added dropwise a solution of bromine (4.41 mL, 86 mmol), and the mixture was stirred for 15 h at 20 °C. The organic layer was washed with aq Na₂S₂O₃ and dried (MgSO₄). After evaporation of the solvent, the crude product was purified by column chromatography (heptane) to yield 24.16 g (97%) of **22a**; ¹H NMR (200.13 MHz, CDCl₃) δ 7.52 (d, J = 8.6, 2H), 7.45 (dd, J = 8.6, 1.8, 2H), 7.44 (d, J = 1.8, 2H), 1.90 (m, 4H), 1.32-0.99 (m, 24H), 0.84 (t, J = 6.8, 6H), 0.57 (m, 4H); ¹³C NMR (50.32

MHz, CDCl₃) δ 152.5, 139.0, 130.1, 126.1, 121.4, 121.1, 55.6, 40.1, 31.8, 29.8, 29.4, 29.2, 23.6, 22.6, 14.1; HRMS (LSIMS⁺, mNBA) calcd for C₃₁H₄₄⁷⁹Br₂ (M⁺) m/z 574.1810, found 574.1820; elemental analysis calcd (%) for C₃₁H₄₄Br₂ (576.50): C 64.59, H 7.69; found: C 64.96, H 7.95.

9,9-Dinonyl-9H-fluorene-2,7-dicarboxaldehyde (22b): A solution of 11.65 g (20.21 mmol) of **22a** in 340 mL of anhyd benzene was cooled to 0 °C before 48.5 mL of a solution of *n*-butyllithium (2.5 M in hexane, 121.25 mmol) was added dropwise. After the addition was complete, the reaction mixture was stirred at 60 °C for 4 h, cooled to 0 °C, and *N*-formylpiperidine (32 g, 282.8 mmol) was added and allowed to react at 20 °C for 14 h. Thereafter, 3 M HCl (240 mL) was added. The two layers were separated and the organic layer was washed with water. The solvents were removed under reduced pressure, and the residue was purified by column chromatography (heptane/CH₂Cl₂, gradient from 95:5 to 70:30) to yield 4.65 g (48%) of **22b**; ¹H NMR (200.13 MHz, CDCl₃) δ 10.10 (s, 2H), 7.92 (m, 6H), 2.07 (m, 4H), 1.32-0.97 (m, 24H), 0.82 (t, J = 6.7, 6H), 0.56 (m, 4H); ¹³C NMR (50.32 MHz, CDCl₃) δ 191.6, 152.5, 145.3, 136.2, 129.8, 123.2, 121.0, 55.2, 39.7, 31.4, 29.5, 29.1, 28.9, 28.8, 23.5, 22.3, 13.7; HRMS (LSIMS⁺, mNBA) calcd for C₃₃H₄₇O₂ ([M+H]⁺) m/z 475.3576, found 475.3576; elemental analysis calcd (%) for C₃₃H₄₆O₂ (474.73): C 83.49, H 9.77; found: C 83.65, H 9.86.

2,7-Bis[(1E)-2-(4-methoxyphenyl)ethenyl]-9,9-dinonyl-9H-fluorene (23): To a solution of **22b** (122.0 mg, 0.26 mmol) and 4-(methoxybenzyl)triphenylphosphonium bromide^[119] (261.8 mg, 0.57 mmol) in anhyd CH₂Cl₂ (5 mL), was added *t*-BuOK (87 mg, 0.77 mmol). The mixture was stirred at 20 °C for 48 h. After addition of water, extraction with CH₂Cl₂, and drying (Na₂SO₄), the solvent was evaporated. The residue was purified by filtration through a short pad of silica gel (CH₂Cl₂), to afford a mixture of isomers, which was dissolved in Et₂O (5 mL). A catalytic amount of I₂ was then added and the solution was stirred at 20 °C for 3 h under light exposure (75 W lamp). The organic layer was washed with aq Na₂S₂O₃ and dried (Na₂SO₄). After evaporation of the solvent, the crude product was purified by column chromatography (heptane/AcOEt 98:2 then 95:5) to yield 130.7 mg (75%) of **23**; ¹H NMR (200.13 MHz, CDCl₃) δ 7.65 (d, J = 7.8, 2H), 7.51 and 6.93 (AA'XX', J_{AX} = 8.8, 8H), 7.48 (d, J = 7.8, 2H), 7.46 (s, 2H), 7.16 (d, J = 16.4, 2H), 7.07 (d, J = 16.4, 2H), 3.85 (s, 6H), 2.02 (m, 4H), 1.27-1.08 (m, 24H), 0.82 (t, J = 6.6, 6H), 0.69 (m, 4H); ¹³C NMR (75.48 MHz, CDCl₃) δ 159.2, 151.4, 140.3, 136.5, 130.3, 127.6, 127.4, 127.3, 125.3, 120.4, 119.8, 114.1,

55.2, 54.9, 40.5, 31.8, 30.0, 29.5, 29.24, 29.21, 23.7, 22.6, 14.0; HRMS (ES⁺) calcd for C₄₉H₆₂NaO₂ ([M+Na]⁺) *m/z* 705.4647, found 705.4640; elemental analysis calcd (%) for C₄₉H₆₂O₂ (683.03): C 86.17, H 9.15; found: C 85.53, H 9.14.

4,4'-[(9,9-Dinonyl-9H-fluorene-2,7-diyl)di-(1E)-2,1-ethenediyl]bis(N,N-dibutylbenzenamine) (24) and 7-[(1E)-2-[4-(dibutylamino)phenyl]ethenyl]-9,9-dinonyl-9H-fluorene-2-carboxaldehyde (25): To a solution of **22b** (2 g, 4.21 mmol) and **3a**^[94] (2.56 g, 4.21 mmol) in anhyd CH₂Cl₂ (50 mL), was added *t*-BuOK (709 mg, 6.32 mmol). The mixture was stirred at 20 °C for 16 h. After addition of water, extraction with CH₂Cl₂, and drying (Na₂SO₄), the solvent was evaporated. The residue was filtered through a short pad of silica gel (CH₂Cl₂), to afford a mixture, which was dissolved in Et₂O (65 mL). A catalytic amount of I₂ was then added and the solution was stirred at 20 °C for 16 h under light exposure (75 W lamp). The organic layer was washed with aq Na₂S₂O₃ and dried (Na₂SO₄). After evaporation of the solvent, the compounds were separated by column chromatography (heptane/CH₂Cl₂, gradient from 100:0 to 70:30) to yield 430 mg (12%) of **24** and 1.68 g (59%) of **25**.

24: mp 62 °C; ¹H NMR (200.13 MHz, CDCl₃) δ 7.60 (d, *J* = 8.0, 2H), 7.43 (d, *J* = 8.0, 2H), 7.41 (s, 2H), 7.40 and 6.63 (AA'XX', *J*_{AX} = 8.8, 8H), 7.09 (d, *J* = 16.3, 2H), 6.95 (d, *J* = 16.3, 2H), 3.30 (m, 8H), 1.99 (m, 4H), 1.58 (m, 8H), 1.37 (m, 8H), 1.24-1.06 (m, 24H), 0.97 (t, *J* = 7.2, 12H), 0.81 (t, *J* = 6.5, 6H), 0.69 (m, 4H); ¹³C NMR (50.32 MHz, CDCl₃) δ 151.3, 147.6, 139.8, 137.0, 128.0, 127.6, 124.9, 124.7, 124.3, 120.0, 119.5, 111.6, 54.8, 50.7, 40.6, 31.8, 30.1, 29.53, 29.47, 29.2, 23.7, 22.6, 20.3, 14.05, 13.99; HRMS (LSIMS⁺, mNBA) calcd for C₆₃H₉₂N₂ (M⁺) *m/z* 876.7261, found 876.7258.

25: mp 77 °C; ¹H NMR (200.13 MHz, CDCl₃) δ 10.04 (s, 1H), 7.85 (d, *J* = 1.5, 1H), 7.84 (dd, *J* = 8.2, 1.5, 1H), 7.78 (d, *J* = 8.2, 1H), 7.71 (d, *J* = 8.0, 1H), 7.49 (d, *J* = 8.0, 1H), 7.44 (s, 1H), 7.41 and 6.64 (AA'XX', *J*_{AX} = 8.9, 4H), 7.14 (d, *J* = 16.2, 1H), 6.96 (d, *J* = 16.2, 1H), 3.30 (m, 4H), 2.02 (m, 4H), 1.60 (m, 4H), 1.37 (m, 4H), 1.24-1.04 (m, 24H), 0.97 (t, *J* = 7.2, 6H), 0.82 (t, *J* = 6.6, 6H), 0.62 (m, 4H); ¹³C NMR (50.32 MHz, CDCl₃) δ 192.0, 152.6, 151.5, 147.8, 147.4, 139.2, 137.9, 134.8, 130.5, 129.4, 127.8, 125.1, 124.2, 123.5, 122.7, 121.0, 120.1, 119.5, 111.5, 55.0, 50.6, 40.2, 31.7, 29.8, 29.4, 29.1, 26.3, 23.6, 22.5, 20.2, 14.0. 13.9; HRMS (LSIMS⁺, mNBA) calcd for C₄₈H₆₉NO (M⁺) *m/z* 675.5379, found 675.5379.

2,7-Bis[(1E)-2-[4-(methylsulfonyl)phenyl]ethenyl]-9,9-dinonyl-9H-fluorene (26a): To a solution of **22b** (237 mg, 0.499 mmol) and **9a**^[98] (337 mg, 1.1 mmol) in anhyd THF (15 mL),

was added NaH (60 mg, 60% dispersion in mineral oil). The mixture was stirred at 20 °C for 16 h. After addition of water, extraction with CH₂Cl₂, and drying (Na₂SO₄), the solvent was evaporated. The residue was purified by filtration through a short pad of silica gel (CH₂Cl₂), to yield 370 mg (95%) of **26a**: mp 152-153 °C; ¹H NMR (200.13 MHz, CDCl₃) δ 7.94 and 7.71 (AA'XX', J_{AX} = 8.3, 8H), 7.71 (d, J = 8.2, 2H), 7.54 (d, J = 8.1, 2H), 7.51 (s, 2H), 7.36 (d, J = 16.3, 2H), 7.19 (d, J = 16.3, 2H), 3.09 (s, 6H), 2.04 (m, 4H), 1.25-1.01 (m, 24H), 0.79 (t, J = 6.6, 6H), 0.63 (m, 4H); ¹³C NMR (50.32 MHz, CDCl₃) δ 151.7, 142.9, 141.2, 138.5, 135.4, 133.0, 127.8, 126.8, 126.2, 125.8, 121.1, 120.2, 55.0, 44.5, 40.3, 31.7, 29.9, 29.6, 29.4, 29.1, 23.6, 22.5, 14.0; HRMS (LSIMS⁺, mNBA) calcd for C₄₉H₆₂O₄S₂ (M⁺) *m/z* 778.4090, found 778.4096.

2,7-Bis[(1E)-2-[4-[(1E)-2-[4-(methylsulfonyl)phenyl]ethenyl]phenyl]ethenyl]-9,9-dinonyl-9H-fluorene (26b): To a solution of **22b** (66.5 mg, 0.14 mmol) and **11** (115 mg, 0.28 mmol) in anhyd THF (10 mL), was added NaH (18 mg, 60% dispersion in mineral oil). The mixture was stirred at 20 °C for 16 h and the solvent was removed under reduced pressure. After addition of water, extraction with CH₂Cl₂, and drying (Na₂SO₄), the solvent was evaporated. The residue was purified by column chromatography (CH₂Cl₂) to yield 87 mg (63%) of **26b**; ¹H NMR (200.13 MHz, CDCl₃) δ 7.93 and 7.70 (AA'XX', J_{AX} = 8.5, 8H), 7.69 (d, J = 8.8, 2H), 7.58 (m, 8H), 7.52 (d, J = 8.8, 2H), 7.49 (s, 2H), 7.26 (d, J = 16.3, 2H), 7.25 (s, 4H), 7.16 (d, J = 16.3, 2H), 3.08 (s, 6H), 2.02 (m, 4H), 1.24-1.07 (m, 24H), 0.81 (t, J = 6.7, 6H), 0.67 (m, 4H); HRMS (LSIMS⁺, mNBA) calcd for C₆₅H₇₄O₄S₂ (M⁺) *m/z* 982.5029, found 982.4992.

2,7-Diethenyl-9,9-dinonyl-9H-fluorene (27): To a solution of **22b** (670.0 mg, 1.41 mmol) and methyltriphenylphosphonium iodide (1.46 g, 3.62 mmol) in anhyd THF (32 mL), was added NaH (310 mg, 60% dispersion in mineral oil). The mixture was stirred at 20 °C for 48 h and then filtered through Celite[®] (heptane). After evaporation of the solvent, the crude product was purified by column chromatography (heptane) to yield 417.0 mg (63%) of **27**; ¹H NMR (200.13 MHz, CDCl₃) δ 7.66 (d, J = 7.9, 2H), 7.44 (dd, J = 7.9, J = 1.7, 2H), 7.39 (d, J = 1.7, 2H), 6.84 (dd, J = 17.6, J = 10.9, 2H), 5.84 (dd, J = 17.6, J = 0.9, 2H), 5.30 (dd, J = 10.9, J = 0.9, 2H), 1.58 (m, 4H), 1.29-1.08 (m, 24H), 0.87 (t, J = 6.4, 6H), 0.65 (s, 4H); ¹³C NMR (50.32 MHz, CDCl₃) δ 151.8, 141.1, 137.9, 136.9, 125.7, 120.9, 120.1, 113.4, 55.3, 40.8, 32.3, 30.5, 29.9, 29.7, 24.1, 23.0, 14.5. HRMS (EI) calcd for C₃₅H₅₀ (M⁺) *m/z* 470.3913, found 470.3909.

4,4'-[(9,9-Dinonyl-9H-fluorene-2,7-diyl)di-(1E)-2,1-ethenediyl]dibenzeneamine (28): Air was removed from a solution of **27** (65.9 mg, 0.14 mmol), 4-iodoaniline (**1a**) (77.0 mg, 0.35 mmol) and K₂CO₃ (49.9 mg, 0.36 mmol) in anhyd DMF (3 mL) by blowing argon for 30 min. Then *n*-Bu₄NCl (103.9 mg, 0.37 mmol), PPh₃ (7.5 mg, 0.029 mmol) and Pd(OAc)₂ (3.2 mg, 0.014 mmol) were added. Thereafter, the mixture was stirred at 90 °C for 22 h. The solvent was removed by distillation, and the crude product was purified by column chromatography (heptane/CH₂Cl₂ 30:70 then 25:75) to yield 51.0 mg (56%) of **28**; ¹H NMR (200.13 MHz, CDCl₃) δ 7.62 (d, *J* = 7.9, 2H), 7.44 (d, *J* = 7.9, 2H), 7.42 (s, 2H), 7.38 and 6.70 (AA'XX', *J*_{AX} = 8.5, 8H), 7.10 (d, *J* = 16.4, 2H), 7.00 (d, *J* = 16.4, 2H), 3.68 (br s, 4H), 2.03 (m, 4H), 1.30-1.10 (m, 24H), 0.87 (t, 6H), 0.70 (m, 4H); ¹³C NMR (75.48 MHz, CDCl₃) δ 151.4, 145.9, 140.1, 136.7, 128.4, 127.8, 127.7, 125.8, 125.2, 120.3, 119.7, 115.3, 54.9, 40.6, 31.8, 30.1, 29.5, 29.2, 23.8, 22.8, 22.6, 14.0.; HRMS (LSIMS⁺, mNBA) calcd for C₄₇H₆₀N₂ (M⁺) *m/z* 652.4756, found 652.4733.

9,9-Dinonyl-9H-fluorene-2,7-dimethanol (29a): To a solution of **22b** (1.018 g, 2.14 mmol) in 38 mL of EtOH/CH₂Cl₂ (2/1), was added KBH₄ (346 mg, 6.42 mmol). The mixture was stirred at 20 °C for 14 h. After addition of water, the solvent was evaporated. The residue was filtered and washed with water. The crude product was purified by column chromatography (CH₂Cl₂) to yield 0.994 g (97%) of **29a**; ¹H NMR (200.13 MHz, CDCl₃) δ 7.67 (d, *J* = 8.3, 2H), 7.34 (s, 2H), 7.32 (d, *J* = 8.3, 2H), 4.78 (d, *J* = 5.8, 4H), 1.95 (m, 4H), 1.68 (t, *J* = 5.8, 2H), 1.24-1.03 (m, 24H), 0.83 (t, *J* = 6.7, 6H), 0.60 (m, 4H); ¹³C NMR (50.32 MHz, CDCl₃) δ 151.3, 140.3, 139.7, 125.7, 121.5, 119.6, 65.7, 55.0, 40.3, 31.8, 30.0, 29.5, 29.3, 29.2, 23.8, 22.6, 14.0; HRMS (LSIMS⁺, mNBA) calcd for C₃₃H₅₀O₂ (M⁺) *m/z* 478.3811, found 478.3814; elemental analysis calcd (%) for C₃₃H₅₀O₂ (478.76): C 82.79, H 10.53; found: C 82.81, H 10.56.

2,7-Bis(bromomethyl)-9,9-dinonyl-9H-fluorene (29b): A solution of **29a** (1.05 g, 2.19 mmol) in 48% aq HBr (5.2 mL) was refluxed for 3 h. After addition of aq NaHCO₃, extraction with CH₂Cl₂, and drying (Na₂SO₄), the solvent was evaporated to yield 1.19 g (90%) of **29b**; ¹H NMR (200.13 MHz, CDCl₃) δ 7.64 (d, *J* = 8.2, 2H), 7.36 (d, *J* = 8.2, 2H), 7.34 (s, 2H), 4.60 (s, 4H), 1.94 (m, 4H), 1.25-1.04 (m, 24H), 0.83 (t, *J* = 6.7, 6H), 0.61 (m, 4H); ¹³C NMR (50.32 MHz, CDCl₃) δ 151.6, 140.6, 136.8, 127.9, 123.6, 120.0, 55.1, 40.0, 34.3, 31.8, 29.8, 29.4, 29.1, 23.6, 22.6, 14.1; HRMS (LSIMS⁺, mNBA) calcd for C₃₃H₄₇⁷⁹Br₂ ([M-H]⁺) *m/z* 601.2045, found 601.2026.

[(9,9-Dinonyl-9H-fluorene-2,7-diyl)bis(methylene)]bisphosphonic acid tetraethyl ester (29c): A solution of **29b** (1.18 g, 1.96 mmol) in P(OEt)₃ (20 mL) was refluxed for 60 h. Then P(OEt)₃ was removed by distillation under vacuum. The crude product was purified by column chromatography (CH₂Cl₂/AcOEt, gradient from 85:15 to 50:50) to yield 870 mg (62%) of **29c**; ¹H NMR (200.13 MHz, CDCl₃) δ 7.61 (d, *J* = 8.1, 2H), 7.26 (m, 4H), 4.00 (m, 8H), 3.24 (d, *J* = 21.7, 4H), 1.94 (m, 4H), 1.23 (t, *J* = 7.1, 12H), 1.19-0.98 (m, 24H), 0.83 (t, *J* = 6.7, 6H), 0.57 (m, 4H); ¹³C NMR (50.32 MHz, CDCl₃) δ 151.0, 139.6, 130.2 (d, *J* = 9.1), 128.4 (d, *J* = 6.3), 124.2 (d, *J* = 6.6), 119.6, 62.1 (d, *J* = 7.1), 54.9, 40.4, 34.1 (d, *J* = 137.6), 31.7, 30.1, 29.5, 29.4, 29.2, 23.9, 22.6, 16.1 (d, *J* = 6.1), 14.0; ³¹P NMR (121.50 MHz, CDCl₃) δ 27.15; HRMS (LSIMS⁺, mNBA) calcd for C₄₁H₆₉O₆P₂ ([M+H]⁺) *m/z* 719.4569, found 719.4554.

4,4'-[(9,9-Dinonyl-9H-fluorene-2,7-diyl)bis[(1E)-2,1-ethenediyl-4,1-phenylene-(1E)-2,1-ethenediyl]]bis(N,N-dihexylbenzenamine) (30): To a solution of **29c** (124.4 mg, 0.17 mmol) and **4b** (149.1 mg, 0.38 mmol) in anhyd THF (9 mL), was added NaH (15 mg, 60% dispersion in mineral oil). The mixture was stirred at 20 °C for 20 h and the solvent was removed under reduced pressure. After addition of water, extraction with CH₂Cl₂, and drying (Na₂SO₄), the solvents were evaporated. The residue was purified by column chromatography (heptane/ CH₂Cl₂ 80:20) to yield 82.0 mg (53%) of **30**; ¹H NMR (300.13 MHz, CDCl₃) δ 7.62 (d, *J* = 8.3, 2H), 7.57-7.50 (m, 12H), 7.42 (d, *J* = 8.7, 4H), 7.25 (d, *J* = 16.3, 2H), 7.17 (d, *J* = 16.3, 2H), 7.10 (d, *J* = 16.2, 2H), 6.93 (d, *J* = 16.2, 2H), 6.66 (d, *J* = 8.7, 4H), 3.32 (m, 8H), 2.07 (m, 4H), 1.64 (m, 8H), 1.37 (m, 24H), 1.18-1.10 (m, 24H), 0.96 (t, *J* = 6.4, 12H), 0.85 (t, *J* = 6.9, 6H), 0.75 (m, 4H); ¹³C NMR (75.48 MHz, CDCl₃) δ 151.5, 147.8, 140.5, 137.6, 136.4, 135.7, 128.8, 128.5, 127.8, 127.7, 126.7, 126.2, 125.5, 124.5, 123.2, 120.7, 120.0, 111.6, 55.0, 51.0, 40.5, 31.8, 31.7, 30.1, 29.5, 29.24, 29.22, 27.3, 26.8, 23.8, 22.7, 22.6, 14.0; HRMS (ES⁺) calcd for C₈₇H₁₂₁N₂ ([M+H]⁺) *m/z* 1193.9530, found 1193.9502.

4,4'-[(9,9-Dinonyl-9H-fluorene-2,7-diyl)bis[(1E)-2,1-ethenediyl-5,2-thiophenediyl-(1E)-2,1-ethenediyl]]bis(N,N-dioctylbenzenamine) (31): To a solution of **29c** (140.5 mg, 0.195 mmol), **6b** (225 mg, 0.496 mmol) and 18-crown-6 (10 mg) in anhyd THF (20 mL), was added NaH (48 mg, 60% dispersion in mineral oil). The mixture was refluxed for 7 h. After addition of water, extraction with CH₂Cl₂, and drying (Na₂SO₄), the solvents were evaporated. The residue was then purified by column chromatography (heptane/CH₂Cl₂ 90:10) to yield 175 mg (68%) of **31**; ¹H NMR (200.13 MHz, CDCl₃) δ 7.63 (d, *J* = 8.1, 2H), 7.43 (d, *J* = 8.1, 2H),

7.41 (s, 2H), 7.33 and 6.61 (AA'XX', $J_{AX} = 8.9$, 8H), 7.24 (d, $J = 15.9$, 2H), 6.97 (d, $J = 15.6$, 2H), 6.95 (d, $J = 15.9$, 2H), 6.94 (d, $J = 3.9$, 2H), 6.86 (d, $J = 3.9$, 2H), 6.83 (d, $J = 15.6$, 2H), 3.28 (m, 8H), 2.00 (m, 4H), 1.59 (m, 8H), 1.30 (m, 40H), 1.15-1.07 (m, 24H), 0.89 (t, $J = 6.5$, 12H), 0.82 (t, $J = 6.7$, 6H), 0.67 (m, 4H); ^{13}C NMR (50.32 MHz, CDCl_3) δ 151.5, 147.8, 143.2, 140.6, 140.5, 136.1, 129.1, 128.3, 127.7, 127.0, 125.4, 125.3, 124.0, 121.4, 120.4, 119.9, 117.0, 111.6, 54.9, 51.0, 31.8, 30.0, 29.53, 29.50, 29.33, 29.26, 29.23, 27.3, 27.2, 22.65, 22.62, 14.10, 14.07; HRMS (LSIMS⁺, mNBA) calcd for $\text{C}_{91}\text{H}_{132}\text{N}_2\text{S}_2$ (M^+) m/z 1316.9832, found 1316.9837; elemental analysis calcd (%) for $\text{C}_{91}\text{H}_{132}\text{N}_2\text{S}_2$ (1318.18): C 82.92, H 10.09, N 2.12, S 4.86; found: C 82.82, H 10.33, N 2.07, S 4.83.

4,4'-[(9,9-Dinonyl-9H-fluorene-2,7-diyl)bis[(1E)-2,1-ethenediyl-7,2-(9,9-dinonyl-9H-fluorenediyl)-(1E)-2,1-ethenediyl]]bis(N,N-dibutylbenzenamine) (32): To a solution of **29c** (200 mg, 0.278 mmol) and **25** (414 mg, 0.612 mmol) in anhyd THF (15 mL), was added NaH (25 mg, 60% dispersion in mineral oil). The mixture was stirred at 20 °C for 16 h and the solvent was removed under reduced pressure. After addition of water, extraction with CH_2Cl_2 , and drying (Na_2SO_4), the solvent was evaporated. The residue was purified by column chromatography (heptane/ CH_2Cl_2 , gradient from 92:8 to 85:15) to yield 410 mg (84%) of **32**; ^1H NMR (300.13 MHz, CDCl_3) δ 7.66 (d, $J = 7.6$, 2H), 7.64 (s, 2H), 7.63 (d, $J = 7.6$, 2H), 7.53 (d, $J = 8.4$, 2H), 7.52 (s, 2H), 7.52 (d, $J = 8.0$, 2H), 7.51 (s, 2H), 7.45 and 6.64 (AA'XX', $J_{AX} = 8.8$, 8H), 7.41 (d, $J = 8.2$, 4H), 7.27 (s, 4H), 7.10 (d, $J = 16.1$, 2H), 6.97 (d, $J = 16.1$, 2H), 3.30 (m, 8H), 2.02 (m, 12H), 1.60 (m, 8H), 1.37 (m, 8H), 1.22-1.07 (m, 72H), 0.97 (t, $J = 7.3$, 12H), 0.81 (t, $J = 6.8$, 18H), 0.68 (m, 12H); ^{13}C NMR (75.48 MHz, CDCl_3) δ 151.5, 151.4, 147.7, 140.8, 140.5, 139.6, 137.3, 136.5, 136.1, 128.6, 128.2, 127.7, 125.7, 125.0, 124.7, 124.3, 120.5, 120.1, 119.8, 111.6, 55.0, 54.9, 50.8, 40.7, 31.7, 30.1, 29.5, 29.3, 29.2, 23.8, 22.6, 20.3, 14.1, 14.0; HRMS (ES⁺, $\text{CH}_2\text{Cl}_2/\text{MeOH}$) calcd for $\text{C}_{129}\text{H}_{185}\text{N}_2$ ($[\text{M}+\text{H}]^+$) m/z 1762.4538, found 1762.4533; elemental analysis calcd (%) for $\text{C}_{129}\text{H}_{184}\text{N}_2$ (1762.89): C 87.89, H 10.52, N 1.59; found: C 88.05, H 10.35, N 1.31.

5,5'-[(9,9-Dinonyl-9H-fluorene-2,7-diyl)di-(1E)-2,1-ethenediyl]bis-2-thiophenecarboxaldehyde (33): To a solution of **22b** (170 mg, 0.237 mmol) and **5b** (100.4 mg, 0.545 mmol) in anhyd THF (22 mL), was added NaH (75 mg, 60% dispersion in mineral oil). The mixture was stirred at 20 °C for 15 h, then at 60 °C for 2 h. After addition of water, extraction with CH_2Cl_2 , and drying (Na_2SO_4), the solvents were evaporated. Purification of the residue by column chromatography (heptane/AcOEt 70:30) afforded the crude acetal,

which was hydrolyzed at 20 °C for 2 h, using 10% HCl (4 mL) in THF (8 mL). Thereafter, THF was evaporated and CH₂Cl₂ was added. The two layers were separated and the organic layer was washed with aq NaHCO₃, dried (Na₂SO₄) and evaporated. The crude product was purified by column chromatography (heptane/AcOEt 80:20) to yield 90 mg (55%) of **33**; ¹H NMR (200.13 MHz, CDCl₃) δ 9.87 (s, 2H), 7.70 (d, *J* = 7.8, 2H), 7.69 (d, *J* = 4.1, 2H), 7.50 (d, *J* = 7.8, 2H), 7.46 (s, 2H), 7.26 (m, 4H), 7.19 (d, *J* = 4.1, 2H), 2.02 (m, 4H), 1.26-1.04 (m, 24 H), 0.80 (t, *J* = 6.5, 6H), 0.61 (m, 4H); ¹H NMR (200.13 MHz, C₆D₆) δ 9.51 (s, 2H), 7.55 (d, *J* = 8.0, 2H), 7.43 (s, 2H), 7.24 (d, *J* = 8.0, 2H), 7.10 (d, *J* = 16.1, 2H), 6.98 (d, *J* = 16.1, 2H), 6.88 (d, *J* = 3.9, 2H), 6.56 (d, *J* = 3.9, 2H), 2.14 (m, 4H), 1.46-0.76 (m, 28H), 0.81 (t, *J* = 6.5, 6H).

1,1'-[(9,9-Dinonyl-9H-fluorene-2,7-diyl)bis[(1E)-2,1-ethenediyl-5,2-

thiophenediyl]]bis(piperidine) (34a): To a solution of **22b** (129.6 mg, 0.27 mmol) and [[5-(1-piperidiny)-2-thienyl]methyl]triphenylphosphonium iodide (357.6 mg, 0.63 mmol) in anhyd CH₂Cl₂ (4 mL), was added *t*-BuOK (92 mg, 0.82 mmol). The mixture was stirred at 20 °C for 48 h. After addition of water, extraction with CH₂Cl₂, and drying (Na₂SO₄), the solvent was evaporated. The residue was purified by filtration through a short pad of silica gel (heptane/CH₂Cl₂ 50:50), to afford a mixture of isomers, which was dissolved in Et₂O (5 mL). A catalytic amount of I₂ was then added and the solution was stirred at 20 °C for 3 h under light exposure (75 W lamp). The organic layer was washed with aq Na₂S₂O₃ and dried (Na₂SO₄). After evaporation of the solvent, the crude product was purified by column chromatography (heptane/AcOEt 99:1 then 99:2) to yield 48.5 mg (22%) of **34a**; ¹H NMR (200.13 MHz, CDCl₃) δ 7.64 (d, *J* = 7.9, 2H), 7.49 (d, *J* = 7.9, 2H), 7.41 (s, 2H), 7.21 (d, *J* = 16.5, 2H), 7.18 (d, *J* = 5.7, 2H), 6.97 (d, *J* = 16.5, 2H), 6.92 (d, *J* = 5.7, 2H), 2.97 (m, 8H), 1.98 (m, 4H), 1.78 (m, 8H), 1.59 (m, 4H), 1.25-1.07 (m, 24 H), 0.81 (t, *J* = 6.6, 6H), 0.72 (m, 4H); ¹³C NMR (50.32 MHz, CDCl₃) δ 156.4, 151.5, 140.1, 136.9, 127.3, 127.2, 124.8, 124.1, 120.8, 120.7, 119.7, 117.2, 56.3, 54.8, 40.4, 31.8, 30.1, 29.6, 29.3, 29.2, 26.1, 23.9, 22.6, 14.1; HRMS (LSIMS⁺, mNBA) calcd for C₅₃H₇₂N₂S₂ (M⁺) *m/z* 800.5137, found 800.5149; elemental analysis calcd (%) for C₅₃H₇₂N₂S₂ (801.30): C 79.44, H 9.06, N 3.50, S 8.00; found: C 79.66, H 9.42, N 3.22, S 7.70.

1,1'-[(9,9-Dinonyl-9H-fluorene-2,7-diyl)bis[(1E)-2,1-ethenediyl-5,2-thiophenediyl-(1E)-2,1-ethenediyl-5,2-thiophenediyl]]bis(piperidine) (34b): Reaction of **33** (77.0 mg, 0.11 mmol) with [[5-(1-piperidiny)-2-thienyl]methyl]triphenylphosphonium iodide (140.0 mg,

0.25 mmol), as described for **34a**, with subsequent purification by column chromatography (heptane/CH₂Cl₂ gradient from 70:30 to 40:60), afforded 20.2 mg (18%) of **34b**; ¹H NMR (300.13 MHz, CDCl₃) δ 7.64 (d, *J* = 8.0, 2H), 7.45 (d, *J* = 8.0, 2H), 7.41 (s, 2H), 7.25 (d, *J* = 15.9, 2H), 7.08 (d, *J* = 5.4, 2H), 6.99 (d, *J* = 15.9, 2H), 6.98 (s, 4H), 6.96 (d, *J* = 3.8, 2H) 6.89 (d, *J* = 3.8, 2H), 6.85 (d, *J* = 5.4, 2H), 2.95 (m, 8H), 2.00 (m, 4H), 1.80 (m, 8H), 1.59 (m, 4H), 1.26-1.05 (m, 24H), 0.82 (t, *J* = 6.8, 6H), 0.66 (m, 4H); ¹³C NMR (75.48 MHz, CDCl₃) δ 156.8, 151.6, 142.9, 141.4, 140.6, 136.0, 128.7, 127.0, 126.6, 126.1, 125.4, 123.9, 121.6, 121.3, 120.5, 120.0, 119.9, 116.4, 56.3, 55.0, 40.6, 31.8, 30.1, 29.5, 29.3, 29.2, 26.2, 23.9, 23.8, 22.6, 14.1; HRMS (ES⁺, MeOH) calcd for C₆₅H₈₁N₂S₄ ([M+H]⁺) *m/z* 1017.5283, found 1017.5268.

Acknowledgments

We acknowledge financial support from Rennes Métropole and Délégation Générale pour l'Armement (DGA Grant 00.34.070.00.470.75.653). L.P. and M.C. received fellowships from MENESR and DGA, respectively. We wish to thank M. H. V. Werts for important help in TPEF experiments, B. K. G. Bhatthula, K. Rousseau, A. Le Cornec and D. Béret for assistance in the synthesis.

References and notes

- [1] R. R. Birge, *Acc. Chem. Res.* **1986**, *19*, 138-146.
- [2] S. Shima, R. P. Ilagan, N. Gillespie, B. J. Sommer, R. G. Hiller, F. P. Sharples, H. A. Frank, R. R. Birge, *J. Phys. Chem. A* **2003**, *107*, 8052-8066.
- [3] D. A. Parthenopoulos, P. M. Rentzepis, *Science* **1989**, *245*, 843-845.
- [4] J. H. Strickler, W. W. Webb, *Opt. Lett.* **1991**, *16*, 1780-1782.
- [5] A. S. Dvornikov, P. M. Rentzepis, *Opt. Commun.* **1995**, *119*, 341-346.
- [6] K. D. Belfield, K. J. Schafer, *Chem. Mater.* **2002**, *14*, 3656-3662.
- [7] K. D. Belfield, Y. Liu, R. A. Negres, M. Fan, G. Pan, D. J. Hagan, F. E. Hernandez, *Chem. Mater.* **2002**, *14*, 3663-3667.
- [8] S. Maruo, O. Nakamura, S. Kawata, *Opt. Lett.* **1997**, *22*, 132-134.
- [9] B. H. Cumpston, S. P. Ananthavel, S. Barlow, D. L. Dyer, J. E. Ehrlich, L. L. Erskine, A. A. Heikal, S. M. Kuebler, I.-Y. S. Lee, D. McCord-Maughon, J. Qin, H. Röckel, M. Rumi, X. L. Wu, S. R. Marder, J. W. Perry, *Nature* **1999**, *398*, 51-54.
- [10] S. Kawata, H.-B. Sun, T. Tanaka, K. Takada, *Nature* **2001**, *412*, 697-698.
- [11] W. Zhou, S. M. Kuebler, K. L. Braun, T. Yu, J. K. Cammack, C. K. Ober, J. W. Perry, S. R. Marder, *Science* **2002**, *296*, 1106-1109.
- [12] J. D. Bhawalkar, G. S. He, C.-K. Park, C. F. Zhao, G. Ruland, P. N. Prasad, *Opt. Commun.* **1996**, *124*, 33-37.
- [13] A. Abbotto, L. Beverina, R. Bozio, S. Bradamante, C. Ferrante, G. A. Pagani, R. Signorini, *Adv. Mater.* **2000**, *12*, 1963-1967.
- [14] W. Denk, J. H. Strickler, W. W. Webb, *Science* **1990**, *248*, 73-76.
- [15] C. Xu, W. Zipfel, J. B. Shear, R. M. Williams, W. W. Webb, *Proc. Natl. Acad. Sci. U. S. A.* **1996**, *93*, 10763-10768.
- [16] D. R. Larson, W. R. Zipfel, R. M. Williams, S. W. Clark, M. P. Bruchez, F. W. Wise, W. W. Webb, *Science* **2003**, *300*, 1434-1437.
- [17] W. Denk, P. B. Detwiler, *Proc. Natl. Acad. Sci. U. S. A.* **1999**, *96*, 7035-7040.
- [18] J. D. Bhawalkar, N. D. Kumar, C. F. Zhao, P. N. Prasad, *J. Clin. Laser Med. Surg.* **1997**, *15*, 201-204.
- [19] D. W. Piston, M. S. Kirby, H. Cheng, W. J. Lederer, W. W. Webb, *Appl. Opt.* **1994**, *33*, 662-669.
- [20] S. Charpak, J. Mertz, E. Beaurepaire, L. Moreaux, K. Delaney, *Proc. Natl. Acad. Sci. U. S. A.* **2001**, *98*, 1230-1234.
- [21] M. Wachowiak, W. Denk, W. Friedrich Rainer, *Proc. Natl. Acad. Sci. U. S. A.* **2004**, *101*, 9097-9102.
- [22] M. Taki, J. L. Wolford, T. V. O'Halloran, *J. Am. Chem. Soc.* **2004**, *126*, 712-713.
- [23] C. J. Chang, E. M. Nolan, J. Jaworski, K. Okamoto, Y. Hayashi, M. Sheng, S. J. Lippard, *Inorg. Chem.* **2004**, *43*, 6774-6779.
- [24] W. R. Zipfel, R. M. Williams, R. Christie, A. Y. Nikitin, B. T. Hyman, W. W. Webb, *Proc. Natl. Acad. Sci. U. S. A.* **2003**, *100*, 7075-7080.
- [25] Y. P. Meshalkin, *Kvantovaya Elektron.* **1996**, *23*, 551-552.
- [26] G. F. White, K. L. Litvinenko, S. R. Meech, D. L. Andrews, A. J. Thomson, *Photochem. Photobiol. Sci.* **2004**, *3*, 47-55.
- [27] G. S. He, G. C. Xu, P. N. Prasad, B. A. Reinhardt, J. C. Bhatt, R. McKellar, A. G. Dillard, *Opt. Lett.* **1995**, *20*, 435-437.
- [28] G. S. He, J. D. Bhawalkar, C. F. Zhao, P. N. Prasad, *Appl. Phys. Lett.* **1995**, *67*, 2433-2435.

- [29] J. E. Ehrlich, X. L. Wu, I. Y. S. Lee, A. A. Heikal, Z. Y. Hu, H. Röckel, S. R. Marder, J. W. Perry, *Mat. Res. Soc. Symp. Proc.* **1997**, 479, 9-15.
- [30] J. E. Ehrlich, X. L. Wu, I. Y. S. Lee, Z. Y. Hu, H. Röckel, S. R. Marder, J. W. Perry, *Opt. Lett.* **1997**, 22, 1843-1845.
- [31] J. W. Perry, S. Barlow, J. E. Ehrlich, A. A. Heikal, Z. Y. Hu, I. Y. Lee, K. Mansour, S. R. Marder, H. Röckel, M. Rumi, S. Thayumanavan, X. L. Wu, *Nonlinear Opt.* **1999**, 21, 225-243.
- [32] Y. Morel, A. Irimia, P. Najechalski, Y. Kervella, O. Stephan, P. L. Baldeck, C. Andraud, *J. Chem. Phys.* **2001**, 114, 5391-5396.
- [33] R. Anémian, Y. Morel, P. L. Baldeck, B. Paci, K. Kretsch, J.-M. Nunzi, C. Andraud, *J. Mater. Chem.* **2003**, 13, 2157-2163.
- [34] K.-S. Lee, H.-K. Yang, J.-H. Lee, O.-K. Kim, H. Y. Woo, H. Choi, M. Cha, M. Blanchard-Desce, *Proc. SPIE-Int. Soc. Opt. Eng.* **2003**, 4991, 175-182.
- [35] M. G. Silly, L. Porrès, O. Mongin, P.-A. Chollet, M. Blanchard-Desce, *Chem. Phys. Lett.* **2003**, 379, 74-80.
- [36] D. Riehl, N. Izard, L. Vivien, E. Anglaret, E. Doris, C. Ménard, C. Mioskowski, L. Porrès, O. Mongin, M. Charlot, M. Blanchard-Desce, R. Anémian, J.-C. Mulatier, C. Barsu, C. Andraud, *Proc. SPIE-Int. Soc. Opt. Eng.* **2003**, 5211, 124-134.
- [37] N. Izard, C. Menard, D. Riehl, E. Doris, C. Mioskowski, E. Anglaret, *Chem. Phys. Lett.* **2004**, 391, 124-128.
- [38] C. Li, C. Liu, Q. Li, Q. Gong, *Chem. Phys. Lett.* **2004**, 400, 569-572.
- [39] M. Charlot, N. Izard, O. Mongin, D. Riehl, M. Blanchard-Desce, *Chem. Phys. Lett.* **2006**, 417, 297-302.
- [40] O. Mongin, L. Porrès, L. Moreaux, J. Mertz, M. Blanchard-Desce, *Org. Lett.* **2002**, 4, 719-722.
- [41] M. Albota, D. Beljonne, J.-L. Brédas, J. E. Ehrlich, J.-Y. Fu, A. A. Heikal, S. E. Hess, T. Kogej, M. D. Levin, S. R. Marder, D. McCord-Maughon, J. W. Perry, H. Röckel, M. Rumi, G. Subramaniam, W. W. Webb, X.-L. Wu, C. Xu, *Science* **1998**, 281, 1653-1656.
- [42] M. Rumi, J. E. Ehrlich, A. A. Heikal, J. W. Perry, S. Barlow, Z.-Y. Hu, D. McCord-Maughon, T. C. Parker, H. Röckel, S. Thayumanavan, S. R. Marder, D. Beljonne, J.-L. Brédas, *J. Am. Chem. Soc.* **2000**, 122, 9500-9510.
- [43] L. Ventelon, L. Moreaux, J. Mertz, M. Blanchard-Desce, *Chem. Commun.* **1999**, 2055-2056.
- [44] L. Ventelon, S. Charier, L. Moreaux, J. Mertz, M. Blanchard-Desce, *Angew. Chem., Int. Ed.* **2001**, 40, 2098-2101.
- [45] M. H. V. Werts, S. Gmouh, O. Mongin, T. Pons, M. Blanchard-Desce, *J. Am. Chem. Soc.* **2004**, 126, 16294-16295.
- [46] B. A. Reinhardt, L. L. Brott, S. J. Clarson, A. G. Dillard, J. C. Bhatt, R. Kannan, L. Yuan, G. S. He, P. N. Prasad, *Chem. Mater.* **1998**, 10, 1863-1874.
- [47] O.-K. Kim, K.-S. Lee, H. Y. Woo, K.-S. Kim, G. S. He, J. Swiatkiewicz, P. N. Prasad, *Chem. Mater.* **2000**, 12, 284-286.
- [48] L. Ventelon, Y. Morel, P. Baldeck, L. Moreaux, J. Mertz, M. Blanchard-Desce, *Nonlinear Opt.* **2001**, 27, 249-258.
- [49] P. K. Frederiksen, M. Jørgensen, P. R. Ogilby, *J. Am. Chem. Soc.* **2001**, 123, 1215-1221.
- [50] L. Ventelon, L. Moreaux, J. Mertz, M. Blanchard-Desce, *Synth. Met.* **2002**, 127, 17-21.
- [51] S. J. K. Pond, M. Rumi, M. D. Levin, T. C. Parker, D. Beljonne, M. W. Day, J.-L. Brédas, S. R. Marder, J. W. Perry, *J. Phys. Chem. A* **2002**, 106, 11470-11480.

- [52] A. Abbotto, L. Beverina, R. Bozio, A. Facchetti, C. Ferrante, G. A. Pagani, D. Pedron, R. Signorini, *Org. Lett.* **2002**, *4*, 1495-1498.
- [53] M. Blanchard-Desce, *C. R. Physique* **2002**, *3*, 439-448.
- [54] L. Zheng, T. Sassa, A. K. Y. Jen, *Mat. Res. Soc. Symp. Proc.* **2002**, *725*, 219-224.
- [55] O. Mongin, J. Brunel, L. Porrès, M. Blanchard-Desce, *Tetrahedron Lett.* **2003**, *44*, 2813-2816.
- [56] B. Strehmel, A. M. Sarker, H. Detert, *ChemPhysChem* **2003**, *4*, 249-259.
- [57] W. J. Yang, D. Y. Kim, M.-Y. Jeong, H. M. Kim, S.-J. Jeon, B. R. Cho, *Chem. Commun.* **2003**, 2618-2619.
- [58] J. Yoo, S. K. Yang, M.-Y. Jeong, H. C. Ahn, S.-J. Jeon, B. R. Cho, *Org. Lett.* **2003**, *5*, 645-648.
- [59] O. K. Kim, K. S. Lee, Z. Huang, W. B. Heuer, C. S. Paik-Sung, *Opt. Mater.* **2003**, *21*, 559-564.
- [60] N. N. P. Moonen, R. Gist, C. Boudon, J.-P. Gisselbrecht, P. Seiler, T. Kawai, A. Kishioka, M. Gross, M. Irie, F. Diederich, *Org. Biomol. Chem.* **2003**, *1*, 2032-2034.
- [61] M. Halik, W. Wenseleers, C. Grasso, F. Stellacci, E. Zojer, S. Barlow, J.-L. Bredas, J. W. Perry, S. R. Marder, *Chem. Commun.* **2003**, 1490-1491.
- [62] Y. Iwase, K. Kamada, K. Ohta, K. Kondo, *J. Mater. Chem.* **2003**, *13*, 1575-1581.
- [63] D. X. Cao, Z. Q. Liu, Q. Fang, G. B. Xu, G. Xue, G. Q. Liu, W. T. Yu, *J. Organomet. Chem.* **2004**, *689*, 2201-2206.
- [64] W. J. Yang, C. H. Kim, M.-Y. Jeong, S. K. Lee, M. J. Piao, S.-J. Jeon, B. R. Cho, *Chem. Mater.* **2004**, *16*, 2783-2789.
- [65] L. Porrès, C. Katan, O. Mongin, T. Pons, J. Mertz, M. Blanchard-Desce, *J. Mol. Struct.* **2004**, *704*, 17-24.
- [66] G. Xia, P. Lu, X. Xu, G. Xu, *Opt. Mater.* **2004**, *27*, 109-113.
- [67] Z.-Q. Liu, Q. Fang, D.-X. Cao, D. Wang, G.-B. Xu, *Org. Lett.* **2004**, *6*, 2933-2936.
- [68] J. Kawamata, M. Akiba, T. Tani, A. Harada, Y. Inagaki, *Chem. Lett.* **2004**, *33*, 448-449.
- [69] K. D. Belfield, A. R. Morales, B.-S. Kang, J. M. Hales, D. J. Hagan, E. W. Van Stryland, V. M. Chapela, J. Percino, *Chem. Mater.* **2004**, *16*, 4634-4641.
- [70] S. J. K. Pond, O. Tsutsumi, M. Rumi, O. Kwon, E. Zojer, J.-L. Brédas, S. R. Marder, J. W. Perry, *J. Am. Chem. Soc.* **2004**, *126*, 9291-9306.
- [71] H. M. Kim, M.-Y. Jeong, H. C. Ahn, S.-J. Jeon, B. R. Cho, *J. Org. Chem.* **2004**, *69*, 5749-5751.
- [72] S.-i. Kato, T. Matsumoto, T. Ishi-i, T. Thiemann, M. Shigeiwa, H. Gorohmaru, S. Maeda, Y. Yamashita, S. Mataka, *Chem. Commun.* **2004**, 2342-2343.
- [73] L. Porrès, O. Mongin, C. Katan, M. Charlot, B. K. G. Bhatthula, T. Pons, J. Mertz, M. Blanchard-Desce, *J. Nonlinear Opt. Phys.* **2004**, *13*, 451-460.
- [74] G. P. Bartholomew, M. Rumi, S. J. K. Pond, J. W. Perry, S. Tretiak, G. C. Bazan, *J. Am. Chem. Soc.* **2004**, *126*, 11529-11542.
- [75] S. K. Lee, W. J. Yang, J. J. Choi, C. H. Kim, S.-J. Jeon, B. R. Cho, *Org. Lett.* **2005**, *7*, 323-326.
- [76] M. Charlot, L. Porres, C. D. Entwistle, A. Beeby, T. B. Marder, M. Blanchard-Desce, *Phys. Chem. Chem. Phys.* **2005**, *7*, 600-606.
- [77] S.-J. Chung, M. Rumi, V. Alain, S. Barlow, J. W. Perry, S. R. Marder, *J. Am. Chem. Soc.* **2005**, *127*, 10844-10845.
- [78] H. Y. Woo, J. W. Hong, B. Liu, A. Mikhailovsky, D. Korystov, G. C. Bazan, *J. Am. Chem. Soc.* **2005**, *127*, 820-821.
- [79] H. Y. Woo, B. Liu, B. Kohler, D. Korystov, A. Mikhailovsky, G. C. Bazan, *J. Am. Chem. Soc.* **2005**, *127*, 14721-14729.

- [80] G. S. He, L. Yuan, N. Cheng, J. D. Bhawalkar, P. N. Prasad, L. L. Brott, S. J. Clarson, B. A. Reinhardt, *J. Opt. Soc. Am. B* **1997**, *14*, 1079-1087.
- [81] K. D. Belfield, D. J. Hagan, E. W. Van Stryland, K. J. Schafer, R. A. Negres, *Org. Lett.* **1999**, *1*, 1575-1578.
- [82] K. D. Belfield, K. J. Schafer, W. Mourad, B. A. Reinhardt, *J. Org. Chem.* **2000**, *65*, 4475-4481.
- [83] R. Kannan, G. S. He, L. Yuan, F. Xu, P. N. Prasad, A. G. Dombroskie, B. A. Reinhardt, J. W. Baur, R. A. Vaia, L.-S. Tan, *Chem. Mater.* **2001**, *13*, 1896-1904.
- [84] L. Antonov, K. Kamada, K. Ohta, F. S. Kamounah, *Phys. Chem. Chem. Phys.* **2003**, *5*, 1193-1197.
- [85] P. Audebert, K. Kamada, K. Matsunaga, K. Ohta, *Chem. Phys. Lett.* **2003**, *367*, 62-71.
- [86] Z.-q. Liu, Q. Fang, D. Wang, D.-x. Cao, G. Xue, W.-t. Yu, H. Lei, *Chem. Eur. J.* **2003**, *9*, 5074-5084.
- [87] S. Charier, O. Ruel, J.-B. Baudin, D. Alcor, J.-F. Allemand, A. Meglio, L. Jullien, *Angew. Chem., Int. Ed.* **2004**, *43*, 4785-4788.
- [88] Y. Wang, O. Y. H. Tai, C. H. Wang, A. K. Y. Jen, *J. Chem. Phys.* **2004**, *121*, 7901-7907.
- [89] M. Barzoukas, M. Blanchard-Desce, *J. Chem. Phys.* **2000**, *113*, 3951-3959.
- [90] M. Barzoukas, M. Blanchard-Desce, *Nonlinear Opt.* **2001**, *27*, 209-218.
- [91] W.-H. Lee, M. Cho, S.-J. Jeon, B. R. Cho, *J. Phys. Chem. A* **2000**, *104*, 11033-11040.
- [92] C. K pplinger, R. Beckert, *Synthesis* **2002**, 1843-1850.
- [93] H. Meier, R. Petermann, U. Dullweber, *J. Prakt. Chem.* **1998**, *340*, 744-754.
- [94] L. Porr s, B. K. G. Bhatthula, M. Blanchard-Desce, *Synthesis* **2003**, 1541-1544.
- [95] B. L. Feringa, R. Hulst, R. Rikers, L. Brandsma, *Synthesis* **1988**, 316-318.
- [96] A. J. Carpenter, D. J. Chadwick, *Tetrahedron* **1985**, *41*, 3803-3812.
- [97] N. Nemoto, J. Abe, F. Miyata, Y. Shirai, Y. Nagase, *J. Mater. Chem.* **1998**, *8*, 1193-1197.
- [98] A. Ulman, C. S. Willand, W. K hler, D. R. Robello, D. J. Williams, L. Handley, *J. Am. Chem. Soc.* **1990**, *112*, 7083-7090.
- [99] M. S. Wong, Z. H. Li, C. C. Kwok, *Tetrahedron Lett.* **2000**, *41*, 5719-5723.
- [100] S. Takahashi, Y. Kuroyama, K. Sonogashira, N. Hagihara, *Synthesis* **1980**, 627-630.
- [101] A. Helms, D. Heiler, G. McLendon, *J. Am. Chem. Soc.* **1992**, *114*, 6227-6238.
- [102] T. Jeffery, *Tetrahedron* **1996**, *52*, 10113-10130.
- [103] We note that this reduction is not observed in the case of pull-pull systems.
- [104] Although no clear phosphorescence could be observed for compound **31** in methylcyclohexane at 77K, it was found that it has a reasonable quantum yield for the generation of singlet oxygen (0.15 in CHCl₃) indicating the formation of triplet states upon excitation (M. H. V. Werts, C. Frochet, unpublished data).
- [105] Field contribution to the Hammett constant for phenyl: $F = 0.12$; Hansch, C.; Leo, A.; Taft, R. W. *Chem. Rev.* **1991**, *91*, 165-195.
- [106] Resonance contribution to the Hammett constant for phenyl: $R = -0.13$.
- [107] C. Xu, W. W. Webb, *J. Opt. Soc. Am. B* **1996**, *13*, 481-491.
- [108] D. A. Oulianov, I. V. Tomov, A. S. Dvornikov, P. M. Rentzepis, *Opt. Commun.* **2001**, *191*, 235-243.
- [109] H. Rath, J. Sankar, V. PrabhuRaja, T. K. Chandrashekar, A. Nag, D. Goswami, *J. Am. Chem. Soc.* **2005**, *127*, 11608-11609.
- [110] R. Misra, R. Kumar, T. K. Chandrashekar, A. Nag, D. Goswami, *Org. Lett.* **2006**, *8*, 629-631.
- [111] D. Y. Kim, T. K. Ahn, J. H. Kwon, D. Kim, T. Ikeue, N. Aratani, A. Osuka, M. Shigeiwa, S. Maeda, *J. Phys. Chem. A* **2005**, *109*, 2996-2999.

- [112] T. K. Ahn, K. S. Kim, D. Y. Kim, S. B. Noh, N. Aratani, C. Ikeda, A. Osuka, D. Kim, *J. Am. Chem. Soc.* **2006**, 128, 1700-1704.
- [113] G. W. Wheland, *Resonance in Organic Chemistry*, Wiley, New York, **1955**.
- [114] M. G. Kuzyk, *J. Chem. Phys.* **2003**, 119, 8327-8334.
- [115] with normalized TPA cross-section (σ_2/N_e) of 124.5 for compound **31** (Table 2) and 126 for compound **C** of reference 77.
- [116] D. F. Eaton, *J. Photochem. Photobiol. B* **1988**, 2, 523-531.
- [117] J. N. Demas, G. A. Crosby, *J. Phys. Chem.* **1971**, 75, 991-1024.
- [118] M. A. Albota, C. Xu, W. W. Webb, *Appl. Opt.* **1998**, 37, 7352-7356.
- [119] G. R. Pettit, M. P. Grealish, M. K. Jung, E. Hamel, R. K. Pettit, J.-C. Chapuis, J. M. Schmidt, *J. Med. Chem.* **2002**, 45, 2534-2542.
- [120] M. S. Wong, M. Samoc, A. Samoc, B. Luther-Davies, M. G. Humphrey, *J. Mater. Chem.* **1998**, 8, 2005-2009.
- [121] B. Tsuie, J. L. Reddinger, G. A. Sotzing, J. Soloducho, A. R. Katritzky, J. R. Reynolds, *J. Mater. Chem.* **1999**, 9, 2189-2200.
- [122] K. J. L. Paciorek, S. R. Masuda, J. G. Shih, J. H. Nakahara, *J. Fluorine Chem.* **1991**, 53, 233-248.
- [123] J. Brunel, O. Mongin, A. Jutand, I. Ledoux, J. Zyss, M. Blanchard-Desce, *Chem. Mater.* **2003**, 15, 4139-4148.
- [124] E. A. Nodiff, S. Lipschutz, P. N. Craig, M. Gordon, *J. Org. Chem.* **1960**, 25, 60-65.
- [125] V. S. Abramov, N. A. Moskva, *Zh. Obshch. Khim.* **1967**, 37, 2243-2247.

Table 1. Photophysical properties of quadrupolar compounds in toluene

#	Compound			Length (nm)	$\lambda_{\max}^{\text{abs}}$ (nm)	log ϵ_{\max}	FWHM (cm^{-1})	$\lambda_{\max}^{\text{em}}$ (nm)	Stokes shift (cm^{-1})	Φ^a	τ^b (ns)
	End- group	Linker	Core								
13a	NHex ₂	PE	BP	2.4	374	4.92	3800	424	3200	0.90	0.70
16a	NHex ₂	PV	BP	2.3	401	4.92	3900	456	3000	0.84	0.82
13b	NHex ₂	PE ₂	BP	3.8	381	5.03	4250	433	3200	0.82	0.73
14	NOct ₂	PV-PE	BP	3.7	406	5.13	3600	463	3000	0.50	0.74
16b	NHex ₂	PE-PV	BP	3.7	400	5.22	3950	452	2900	0.81	0.79
17a	NOct ₂	PV-FV	BP	3.5	443	5.13	4400	522	3400	0.69	1.25
17b	NHex ₂	PV-TV	BP	3.6	458	5.10	3900	522	2700	0.51	0.85
19a	NHex ₂	PE	FL	2.4	387	4.92	3700	421	2100	0.80	0.74
23	OMe	PV	FL	2.3	381	4.82	3900	415	2200	0.90	0.87
28	NH ₂	PV	FL	2.3	392	4.87	4000	433	2400	0.82	0.83
24	NBu ₂	PV	FL	2.3	415	4.98	3600	457	2200	0.79	0.87
34a	Pip	TV	FL	2.2	387	4.78	3900	484	5200	0.45	1.00
19b	NHex ₂	PE ₂	FL	3.8	387	5.11	4100	433	2700	0.82	0.60
30	NHex ₂	PV ₂	FL	3.6	431	5.13	4000	480	2400	0.85	0.83
20	NOct ₂	PV-PE	FL	3.7	411	5.10	4300	464	2800	0.61	0.80
32	NBu ₂	PV-FIV	FL	4.5	429	5.26	3700	472	2100	0.78	0.73
31	NOct ₂	PV-TV	FL	3.5	470	5.09	3800	525	2200	0.47	0.79
34b	Pip	TV ₂	FL	3.5	451	4.98	3900	540	3600	0.45	0.67
21b	SO ₂ CF ₃	PE	FL	2.4	372	4.84	3900	404	2200	0.98	0.79
21a	SO ₂ Oct	PE	FL	2.4	363	4.86	3500	389	1800	0.76	0.64
26a	SO ₂ Me	PV	FL	2.3	387	4.82	3600	423	2200	0.91	0.87
21c	SO ₂ Oct	PV-PE	FL	3.7	382	5.08	4500	419	2300	0.90	0.56
26b	SO ₂ Me	PV ₂	FL	3.7	412	4.91	4000	456	2300	0.73	0.74

^a Fluorescence quantum yield determined relative to fluorescein in 0.1 M NaOH. ^b Fluorescence lifetime determined using time-correlated single-photon counting (TCSPC).

Table 2. Structure-TPA properties of quadrupolar compounds in toluene

#	Compound			E_{gap}^a (eV)	$2\lambda_{\text{max}}^{\text{OPA}}$ (nm)	$\lambda_{\text{max}1}^{\text{TPA}}$ (nm)	$\lambda_{\text{max}2}^{\text{TPA}}$ (nm)	σ_2 (GM) ^b			N_e^c	σ_2/N_e^d (GM)
	End-group	Linker	Core					at 705 nm	at $\lambda_{\text{max}1}^{\text{TPA}}$	at $\lambda_{\text{max}2}^{\text{TPA}}$		
13a	NHex ₂	PE	BP	3.12	748	-	-	890	-	-	28	31.8
16a	NHex ₂	PV	BP	2.90	802	730	-	740	1040	-	28	37.1
13b	NHex ₂	PE ₂	BP	3.06	762	750	-	610	820	-	44	18.6
14	NOct ₂	PV-PE	BP	2.87	812	815	-	1140	910	-	44	25.9
16b	NHex ₂	PE-PV	BP	2.92	800	740	-	1230	1050	-	44	28.0
17a	NOct ₂	PV-FV	BP	2.59	886	850	-	810	420	-	44	18.4
17b	NHex ₂	PV-TV	BP	2.54	916	880	960	3040	1350	1020	44	69.1
19a	NHex ₂	PE	F1	3.07	774	-	-	1200	-	-	28	42.9
23	OMe	PV	F1	3.12	762	-	-	110	-	-	28	3.9
28	NH ₂	PV	F1	3.01	784	-	-	400	-	-	28	14.3
24	NBu ₂	PV	F1	2.85	830	740	-	1130	1260	-	28	45.0
34a	Pip	TV	F1	2.88	774	-	-	95	-	-	28	3.4
19b	NHex ₂	PE ₂	F1	3.03	774	735	-	1080	1020	-	44	24.5
30	NHex ₂	PV ₂	F1	2.73	862	730	815	2110	1920	1210	44	48.0
20	NOct ₂	PV-PE	F1	2.84	822	815	-	1970	1150	-	44	44.8
32	NBu ₂	PV-FIV	F1	2.76	858	730	-	3470	2960	-	56	62.0
31	NOct ₂	PV-TV	F1	2.50	940	880	-	5480	1530	-	44	124.5
34b	Pip	TV ₂	F1	2.53	902	735	-	850	680	-	44	19.3
21b	SO ₂ CF ₃	PE	F1	3.20	744	730	-	83	68	-	32	2.6
21a	SO ₂ Oct	PE	F1	3.30	726	730	-	52	33	-	32	1.6
26a	SO ₂ Me	PV	F1	3.07	774	-	-	220	-	-	32	6.9
21c	SO ₂ Oct	PV-PE	F1	3.10	764	-	-	610	-	-	48	12.7
26b	SO ₂ Me	PV ₂	F1	2.87	824	725	815	1040	960	420	48	21.7

^a The electronic gap (E_{gap}) is calculated from the absorption and emission maxima. ^b 1 GM = 10^{-50} cm⁴.s.photon⁻¹; TPEF measurements were performed using a mode-locked Ti:sapphire laser delivering 80 fs pulses at 80 MHz, calibrating with fluorescein.^[107] ^b Effective number of π electrons in the conjugated system.^[114] ^c Highest TPA cross-section measured in the 700-1000 nm range, normalized by the effective number N_e of π electrons in the conjugated system.

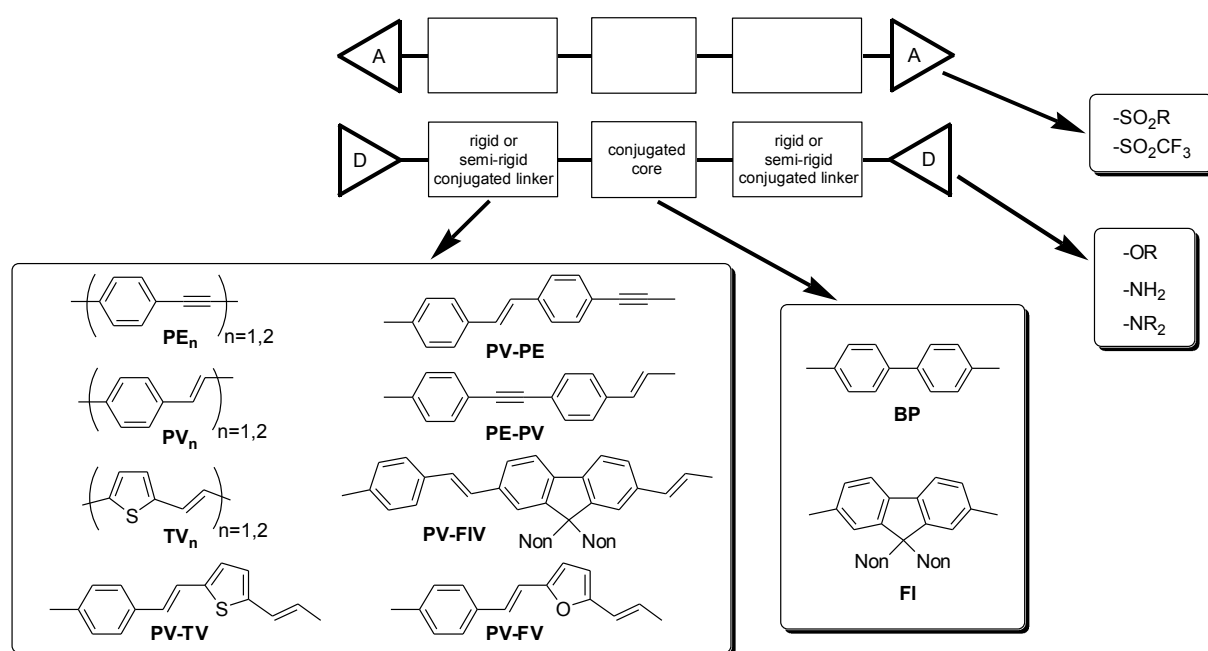
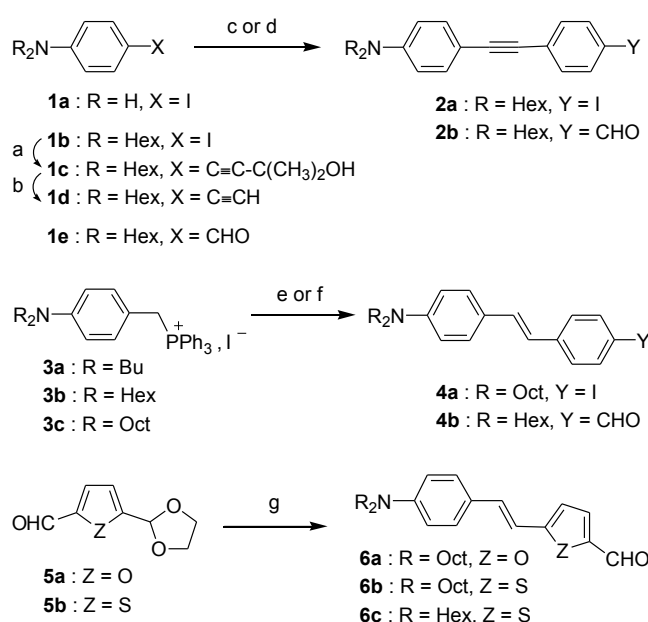
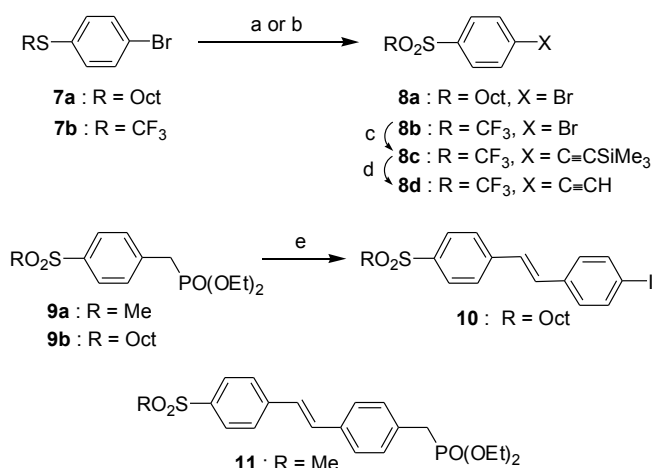


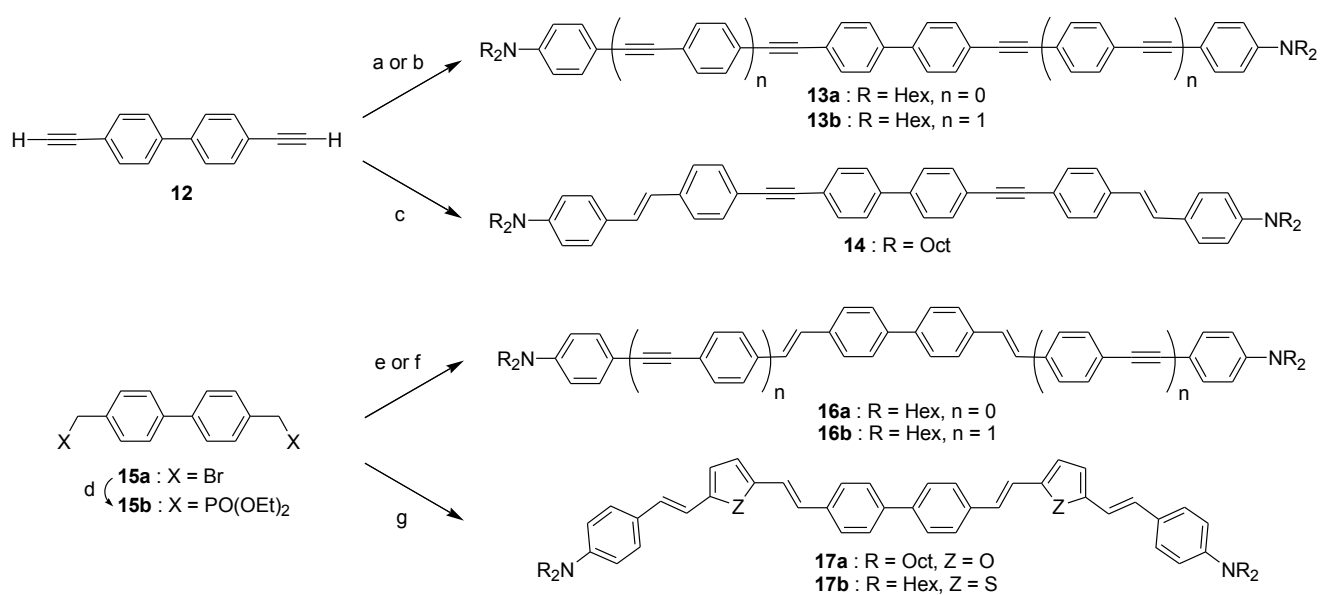
Figure 1. Molecular engineering of pull-pull and push-push fluorophores designed for TPEF.



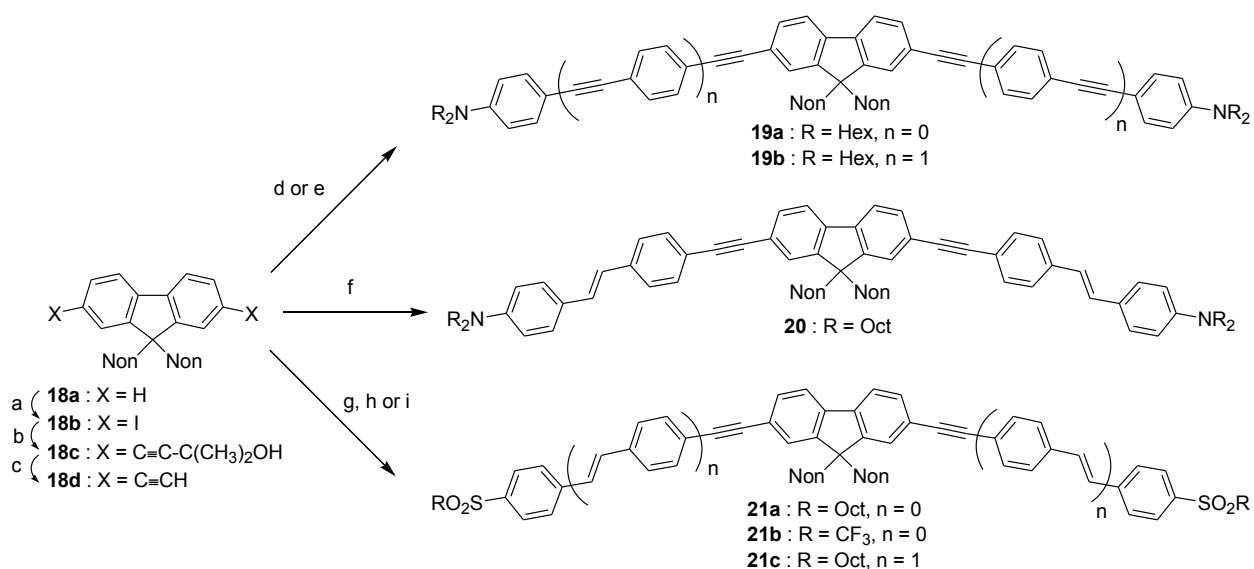
Scheme 1. Reagents and conditions: (a) 2-methyl-3-butyn-2-ol, Pd(PPh₃)₂Cl₂, CuI, Et₃N, 40 °C, 12 h (82%); (b) NaOH, toluene/*i*-PrOH, reflux, 1 h (87%); (c) **1d** (1 equiv), 1,4-diiodobenzene (3 equiv), Pd(PPh₃)₂Cl₂, CuI, toluene/Et₃N, 30 °C, 6 h (71% of **2a**); (d) **1d** (1 equiv), 4-bromobenzaldehyde (1.2 equiv), Pd(PPh₃)₂Cl₂, CuI, toluene/Et₃N, 40 °C, 15 h (74% of **2b**); (e) **3c**, 4-iodobenzaldehyde, *t*-BuOK, CH₂Cl₂, 20 °C, 5 h, then I₂ cat, hv (85% of **4a**); (f) **3b**, terephthalaldehyde mono-(diethylacetal), *t*-BuOK, CH₂Cl₂, 20 °C, 24 h; HCl, 20 °C, 1 h; I₂ cat, hv (84% of **4b**); (g) **3b** or **3c**, conditions as in f (95% of **6a**, 79% of **6b**, 85% of **6c**).



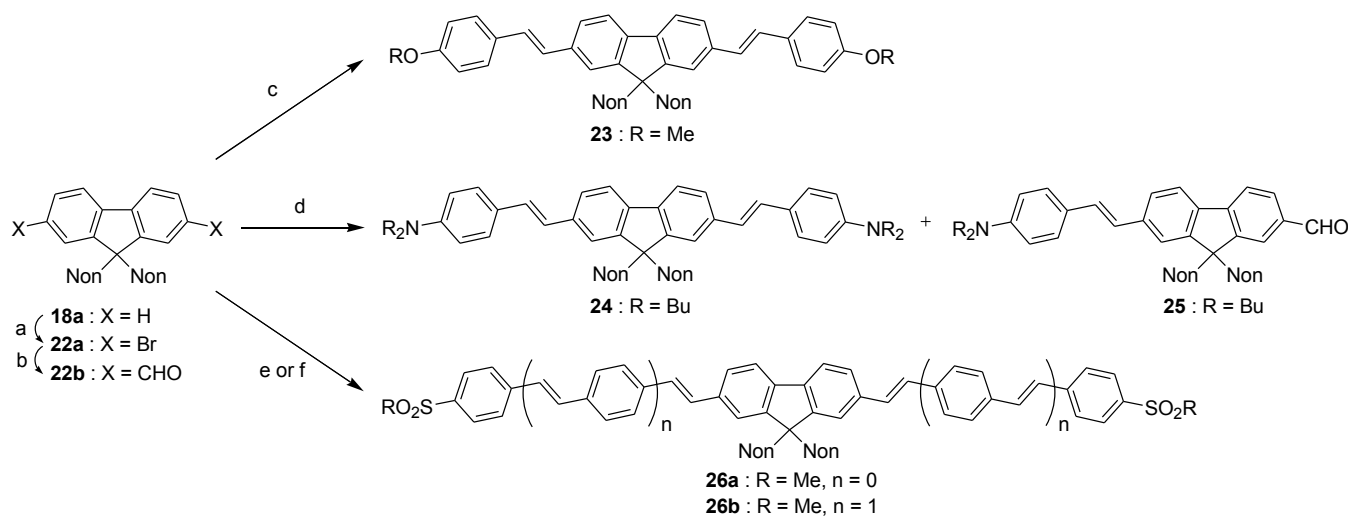
Scheme 2. Reagents and conditions: (a) **7a**, H₂O₂, Na₂WO₄·2H₂O cat, EtOH, reflux, 1 h (93% of **8a**); (b) **7b**, H₂O₂, AcOH, reflux, 3 h (89% of **8b**); (c) HC≡CSiMe₃, Pd(PPh₃)₂Cl₂, CuI, Et₃N, 40 °C, 3 h (88%); (d) TBAF, THF (64%); (e) **9b**, 4-iodobenzaldehyde, NaH, THF, 20 °C, 15 h (61%).



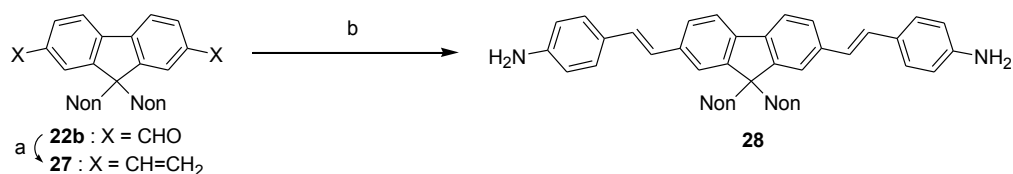
Scheme 3. Reagents and conditions: (a) **1b** (2.3 equiv), Pd(PPh₃)₂Cl₂, CuI, toluene/Et₃N, 20 °C, 2 h (84% of **13a**); (b) **2a**, conditions as in a (86% of **13b**); (c) **4a**, conditions as in a, 3.5 h (81%); (d) P(OEt)₃, toluene, reflux, 60 h (86%); (e) **1e** (2 equiv), NaH, THF, 20 °C, 20 h, then reflux, 4 h (70% of **16a**); (f) **2b** (2.3 equiv), NaH, THF, 18-crown-6 cat, 40 °C, 3 h (84% of **16b**); (g) **6a** or **6c** (2.1 equiv), NaH, THF, 20 °C, 16–19 h (80% of **17a**, 64% of **17b**).



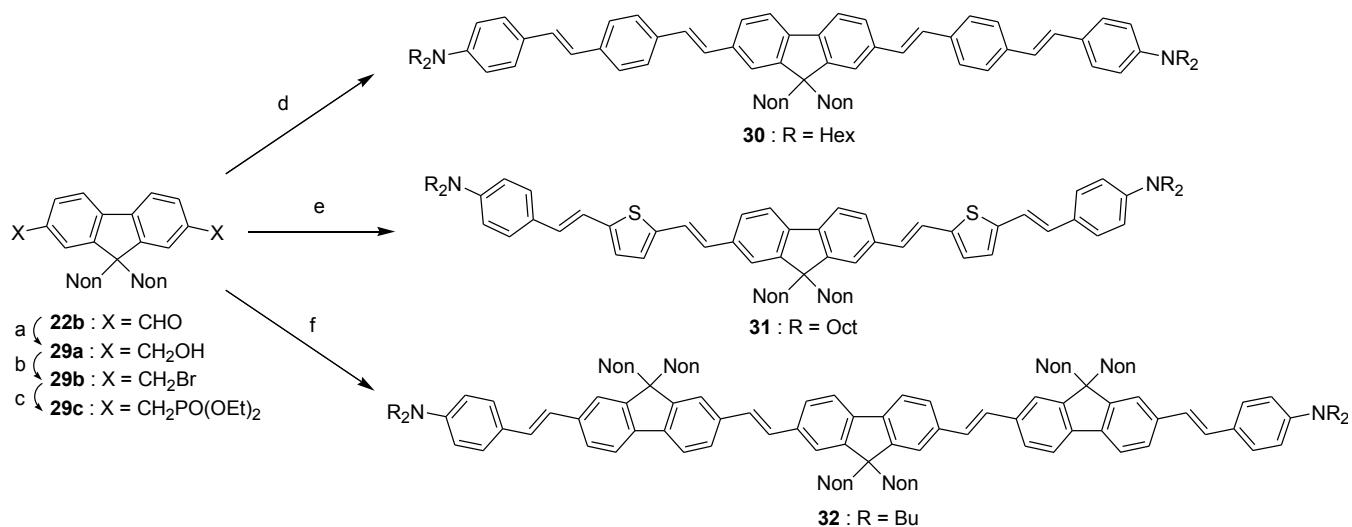
Scheme 4. Reagents and conditions: (a) I₂, H₅IO₆, AcOH, H₂SO₄, H₂O, 75 °C, 2 h (69%); (b) 2-methyl-3-butyn-2-ol, Pd(PPh₃)₂Cl₂, CuI, Et₃N, 20 °C, 16 h (72%); (c) KOH, toluene/*i*-PrOH, reflux, 0.5 h (88%); (d) **1b** (2.4 equiv), Pd(PPh₃)₂Cl₂, CuI, toluene/Et₃N, 20 °C, 3 h (45% of **19a**); (e) **2a**, conditions as in d, 20 h (82% of **19b**); (f) **4a**, conditions as in d, 15 h (83%); (g) **8a**, conditions as in d, 45 °C, 6 h (84% of **21a**); (h) **18b**, **8d** (2.5 equiv), conditions as in d, 40 °C, 14 h (60% of **21b**); (i) **10**, conditions as in d, 35 °C, 14 h (87% of **21c**).



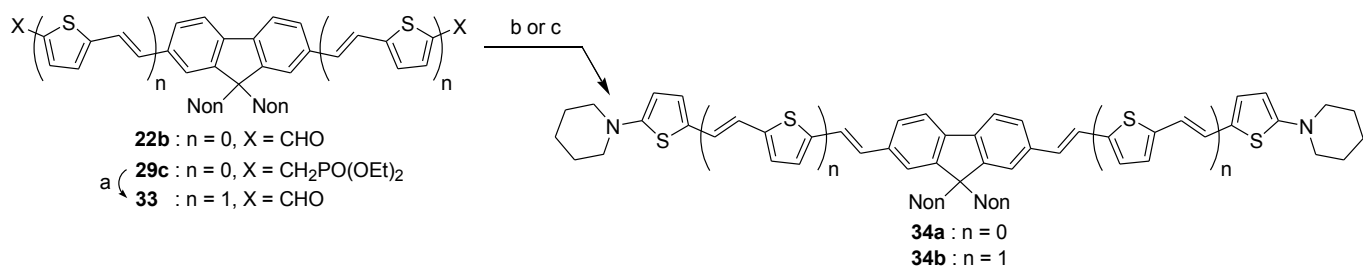
Scheme 5. Reagents and conditions: (a) Br₂ (2 equiv), CH₂Cl₂, 20 °C, 15 h (97%); (b) *n*-BuLi, benzene, 60 °C, 4 h, then *N*-formylpiperidine, 20 °C, 14 h (48%); (c) 4-(methoxybenzyl)triphenylphosphonium bromide (2.2 equiv), *t*-BuOK, CH₂Cl₂, 20 °C, 48 h, then I₂ cat, hv (75%); (d) **3a** (1.0 equiv), *t*-BuOK, CH₂Cl₂, 20 °C, 16 h, then I₂ cat, hv (12% of **24**, 59% of **25**); (e) **9a** (2.2 equiv), NaH, THF, 20 °C, 16 h (95% of **26a**); (f) **11**, conditions as in e (63% of **26b**).



Scheme 6. Reagents and conditions: (a) methyltriphenylphosphonium iodide (2.5 equiv), NaH, THF, 20 °C, 48 h (63%); (b) **1a** (2.5 equiv), Pd(OAc)₂, PPh₃, *n*-Bu₄NCl, K₂CO₃, DMF, 90 °C, 22 h (56%).



Scheme 7. Reagents and conditions: (a) KBH_4 , $\text{EtOH}/\text{CH}_2\text{Cl}_2$, 20°C , 14 h (97%); (b) concd HBr , reflux, 3 h (90%); (c) $\text{P}(\text{OEt})_3$, reflux, 60 h (62%); (d) **4b** (2.2 equiv), NaH , THF , 20°C , 20 h (53%); (e) **6b** (2.5 equiv), NaH , THF , 18-crown-6 cat, reflux, 7 h (68%); (f) **25** (2.2 equiv), NaH , THF , 20°C , 16 h (84%).



Scheme 8. Reagents and conditions: (a) **5b** (2.3 equiv), NaH , THF , 20°C , 15 h, then 60°C , 2 h; HCl , 20°C , 2 h (55%); (b) **22b**, [[5-(1-piperidiny)l-2-thienyl]methyl]triphenylphosphonium iodide (2.3 equiv), $t\text{-BuOK}$, CH_2Cl_2 , 20°C , 48 h, then I_2 cat, $h\nu$ (22% of **34a**); (c) **33**, conditions as in b (18% of **34b**).

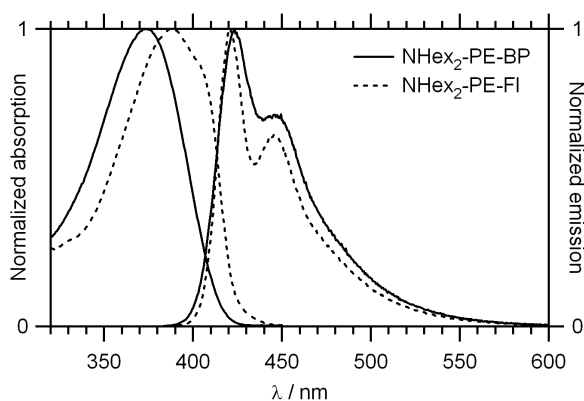


Figure 2. Absorption and emission of **13a** and **19a** in toluene: core effect.

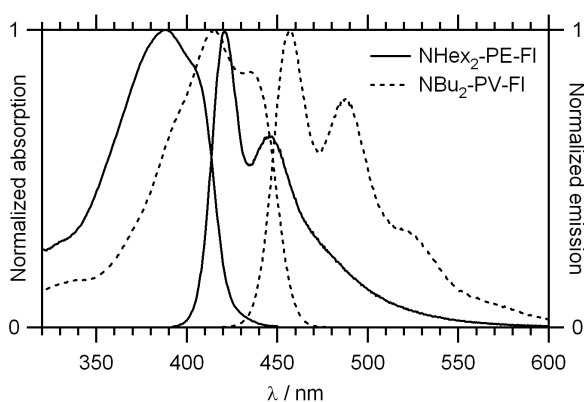


Figure 3. Absorption and emission of **19a** and **24** in toluene: linker effect.

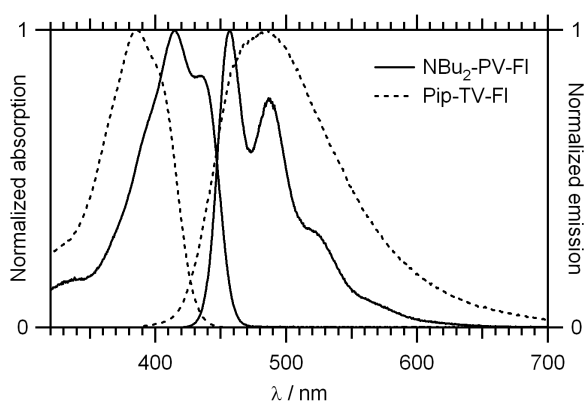


Figure 4a

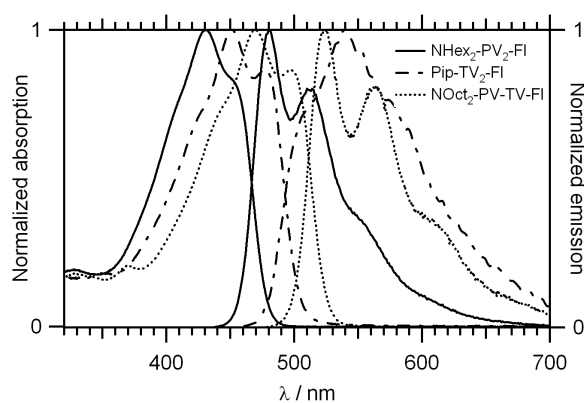


Figure 4b

Figure 4. Absorption and emission in toluene of (a) **24** and **34a**; (b) **30**, **34b** and **31**: connector effects.

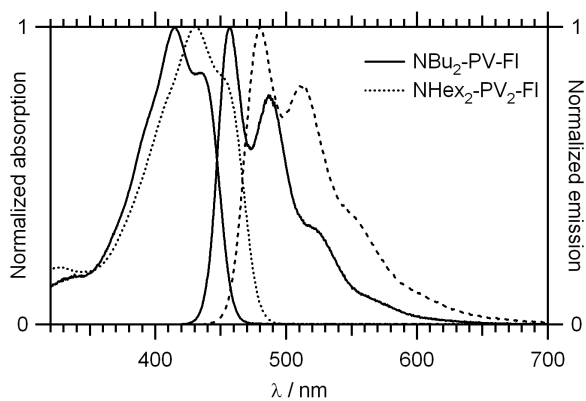


Figure 5a

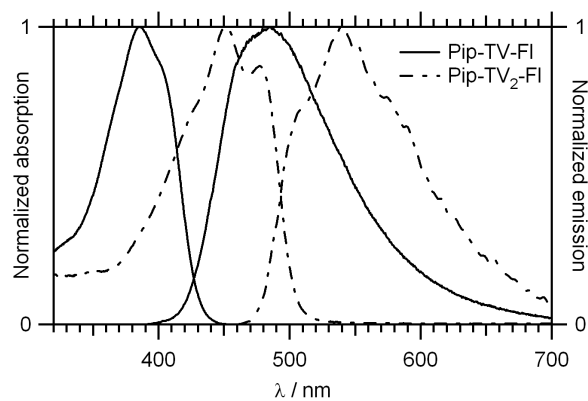


Figure 5b

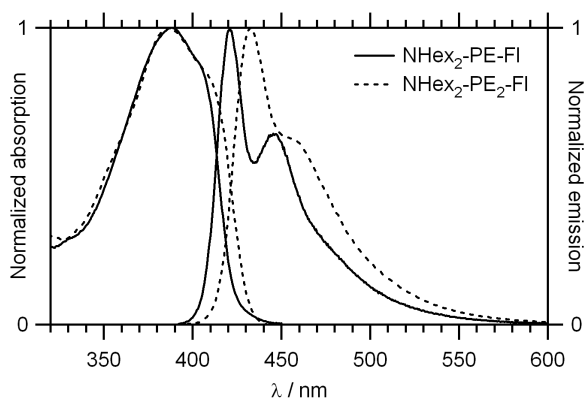


Figure 5c

Figure 5. Absorption and emission spectra in toluene of (a) **24** and **30**; (b) **34a** and **34b**; (c) **19a** and **19b**: length effects.

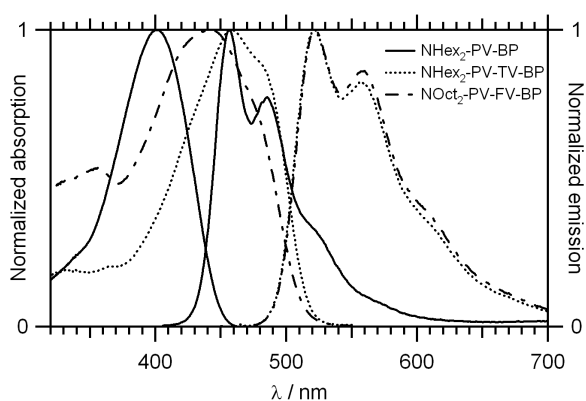


Figure 6a

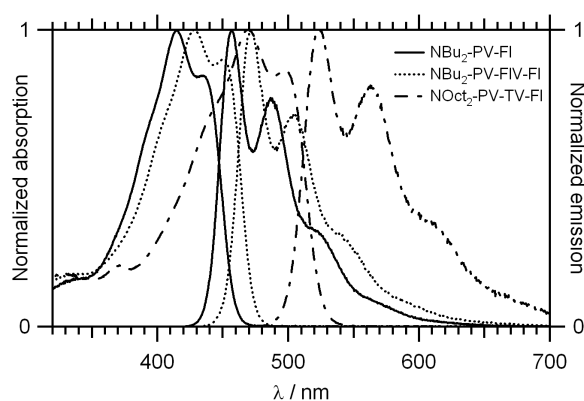


Figure 6b

Figure 6. Absorption and emission spectra in toluene of (a) **16a**, **17b** and **17a**; (b) **24**, **32** and **31**: length effects.

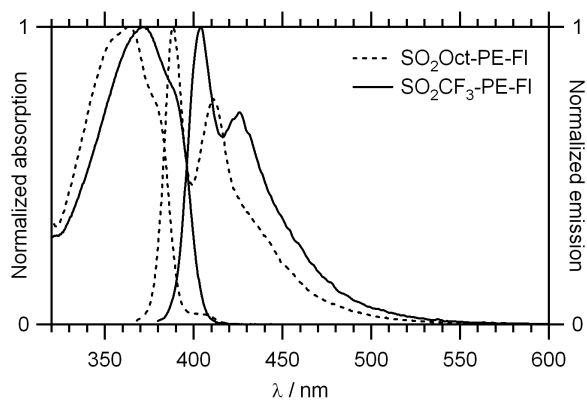


Figure 7a

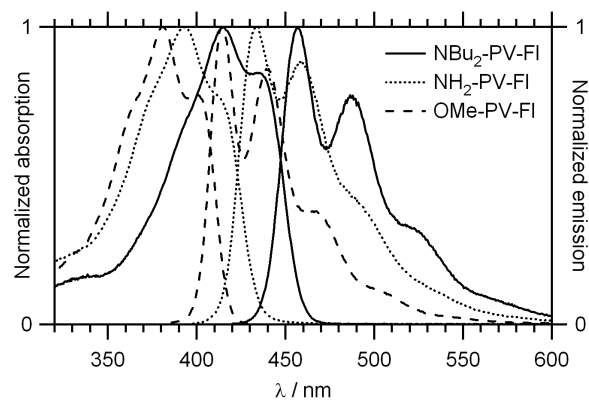


Figure 7b

Figure 7. Absorption and emission spectra in toluene of (a) **21a** and **21b**; (b) **24**, **28** and **23**: end-groups' effects.

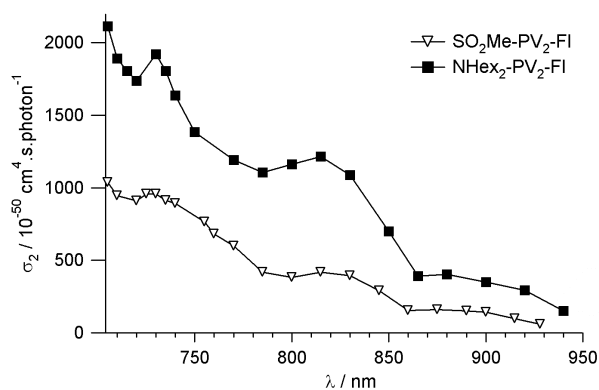


Figure 8. TPA spectra of **26b** and **30** in toluene: end-group (push-push vs pull-pull) effect.

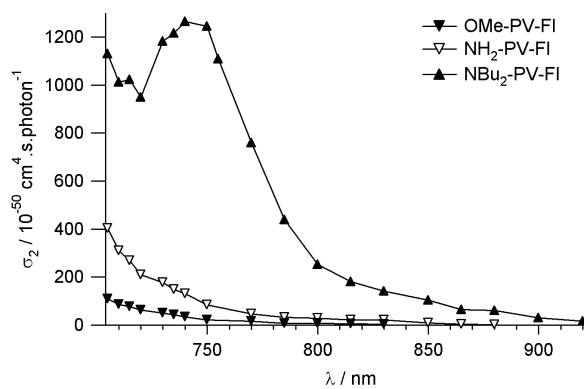


Figure 9. TPA spectra of **23**, **28** and **24** in toluene: donor strength effect.

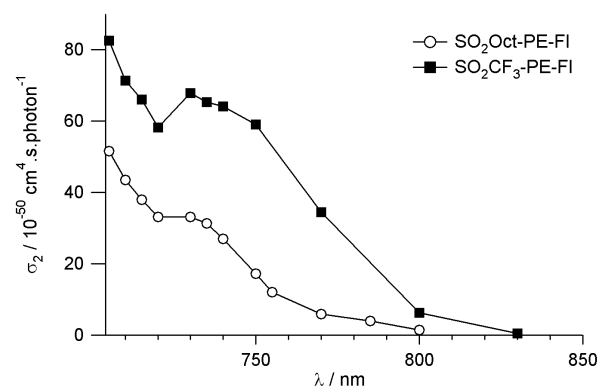


Figure 10. TPA spectra of **21a** and **21b** in toluene: acceptor strength effect.

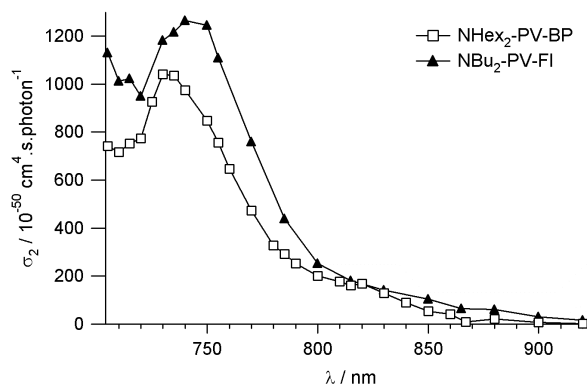


Figure 11. TPA spectra of 16a and 24 in toluene: core effect.

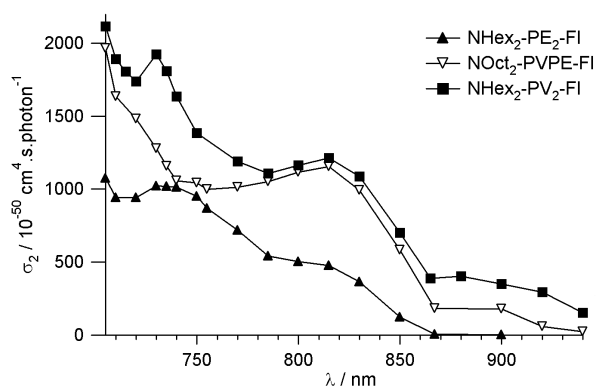


Figure 12. TPA spectra in toluene of 19b, 20 and 30: linker effect.

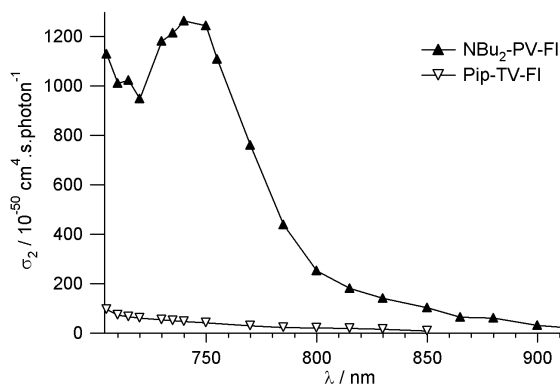


Figure 13a

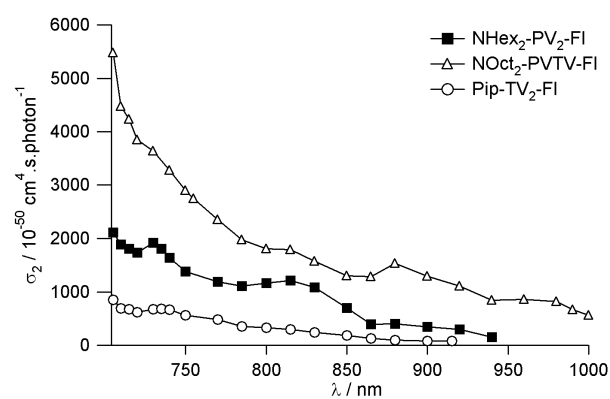


Figure 13b

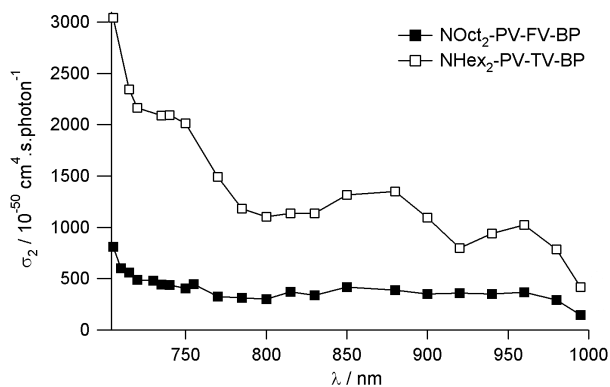


Figure 13c

Figure 13. TPA spectra in toluene of (a) 24 and 34a; (b) 30, 31 and 34b; (c) 17a and 17b: connector effects.

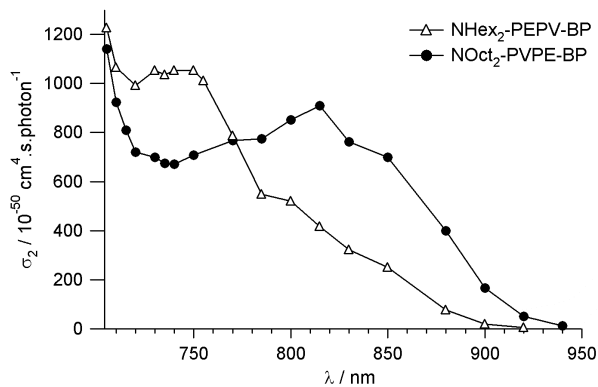


Figure 14. TPA spectra of **16b** and **14** in toluene: topology effect.

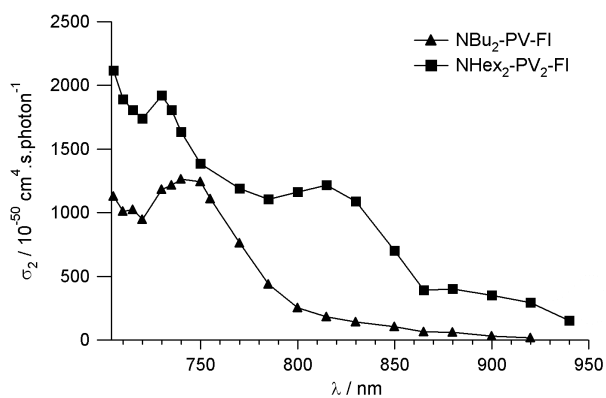


Figure 15a

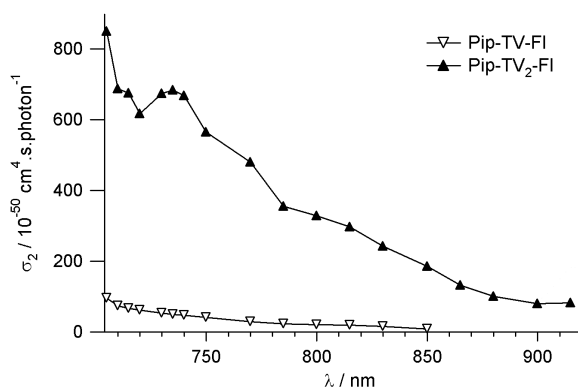


Figure 15b

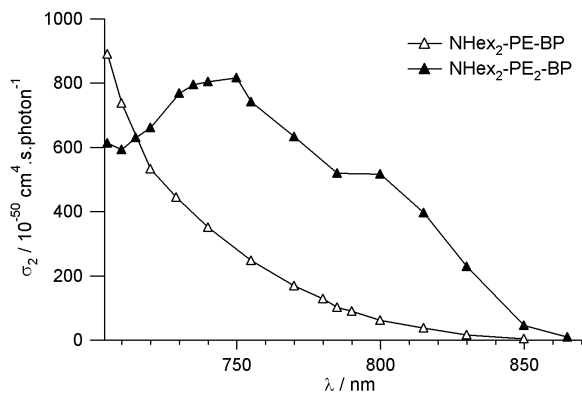


Figure 15c

Figure 15. TPA spectra in toluene of (a) 24 and 30; (b) 34a and 34b; (c) 13a and 13b: length effects.

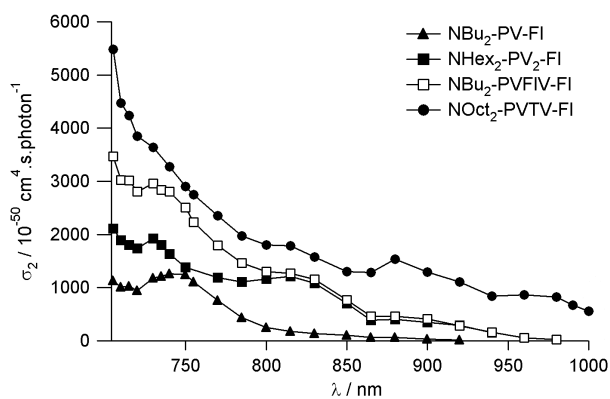
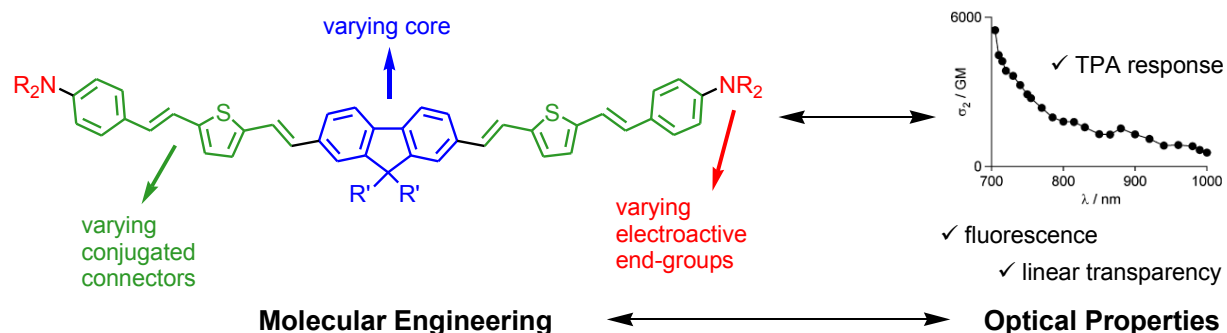


Figure 16. TPA spectra of 24, 30, 32 and 31 in toluene.

Graphical Abstract



A comprehensive series of push-push and pull-pull fluorophores was prepared from the symmetrical functionalization of an ambivalent core with conjugated rods bearing acceptor or donor end-groups. Their absorption, photoluminescence and two-photon absorption (TPA) properties have been investigated, allowing to derive structure-property relationships and to lay guidelines for both spectral tuning and amplification of TPA.